Title
Global atmospheric distributions and source strengths of light hydrocarbons and tetrachloroethene

Journal
Journal of Geophysical Research, 103(D21)

ISSN
0148-0227

Authors
Gupta, Mohan L
Cicerone, Ralph J
Blake, Donald R
et al.

Publication Date
1998-11-20

DOI
10.1029/98jd02645

JOURNAL OF GEOPHYSICAL RESEARCH, VOL. 103, NO. D21, PAGES 28,219–28,235, NOVEMBER 20, 1998

Global atmospheric distributions and source strengths of light hydrocarbons and tetrachloroethene

Mohan L. Gupta[1] and Ralph J. Cicerone
Department of Earth System Science, University of California, Irvine

Donald R. Blake and F. Sherwood Rowland
Department of Chemistry, University of California, Irvine

Ivar S. A. Isaksen
Institute of Geophysics, University of Oslo, Oslo, Norway

Abstract. The atmospheric distributions of CH_4, C_2H_6, C_3H_8, C_2H_2, and C_2Cl_4 and their annual chemical removal rates in steady state are determined versus latitude using a modified version of the Oslo two-dimensional global tropospheric photochemical model. A photochemically calculated hydroxyl radical distribution, which has been validated with methylchloroform data, and seasonally varying surface measurements of the title species are used to compute their respective global annual surface source strengths and steady state lifetimes. Computed annual surface source strengths of CH_4, C_2H_6, C_3H_8, C_2H_2, and C_2Cl_4 are 490, 10.4, 8.4, 3.1 Tg (1 Tg = 10^{12} g), and 432 kT (1 kT = 10^9 g), respectively. The calculated annual chemical removal rates of these compounds show distinct latitudinal distributions. Because their steady state global lifetimes are less than the model interhemispheric exchange time (about 1 year), the calculated north to south ratios of the deduced surface emission strengths of C_2H_6, C_3H_8, C_2H_2, and C_2Cl_4 probably reflect the locations of their sources. Within the limits of previously estimated industrial emissions of C_2Cl_4 (3–4 kT) for the southern hemisphere, our calculations indicate that about 47 kT of additional southern hemispheric source of C_2Cl_4 is required for 1989–1990 to attain steady state mass balance in this region. There are two possibilities for this needed source: either other industrial sources are missing, or there are unidentified natural sources of C_2Cl_4. So far, oceans have been suggested as a natural source. Normalization of monthly varying ratios of hemispherically averaged calculated surface mixing ratios of C_2H_6, C_3H_8, and C_2H_2 and their respective observed mixing ratios with respect to those for C_2Cl_4 indicates that the sources of these hydrocarbons are seasonal in nature. It is also shown that convective transport effectively redistributes these short-lived species but their calculated surface source strengths are relatively independent of this transport process.

1. Introduction

The chemical composition of the Earth's atmosphere and its spatial and temporal variabilities are controlled by coupled photochemical and dynamical processes. This coupling becomes even more complicated by changing biological phenomena [*Prinn*, 1994] and by active exchanges between the Earth's surface and atmosphere. The Earth's atmospheric composition has been continually modified by natural and anthropogenic forces, particularly during the industrial era. Observations of trace gases in the atmosphere have revealed the extent to which the Earth's atmosphere and its oxidative capacity have changed [*Isaksen*, 1988; *Thompson*, 1992; *World Meteorological Organization* (*WMO*), 1994]. Although spatial and temporal variations in methane (CH_4), the most abundant hydrocarbon present in the atmosphere, have been studied extensively, nonmethane hydrocarbons (NMHCs) have received less attention in studies of global atmospheric chemistry. Important roles played by NMHCs in urban photochemical smog, acid deposition, regional and global budgets of CO, OH, O_3, NO_x (defined as NO + NO_2), heterogeneous and nighttime tropospheric photochemistry, and as indicators of air mass age, tracer transport, and halogen radical concentrations have been well documented (see a review by *Singh and Zimmerman* [1992, and references therein]). The *Intergovernmental Panel on Climate Change* (*IPCC*) [1995] report reviewed the indirect climatic importance of NMHCs and NO_x on the radiative balance of the Earth's atmosphere which modify tropospheric O_3 and CH_4 distributions through their nonlinear photochemistry [*Ramanathan et al.*, 1985; *Dickinson and Cicerone*, 1986; *Lin et al.*, 1988; *Sillman et al.*, 1990], but failed to quantify the magnitude of this indirect forcing because of uncertainties in the source strengths and global distributions of NMHCs and NO_x. The uncertainties in the identity of natural and anthropogenic NMHC sources and spatial and temporal variability in their corresponding strengths are mainly due to their relatively reactive nature, and hence their short lifetimes and low abundances [*Singh and Zimmerman*, 1992]. Because of these uncer-

[1]Now at Department of Atmospheric Sciences, University of California, Los Angeles.

Paper number 98JD02645.
0148-0227/98/98JD-02645$09.00

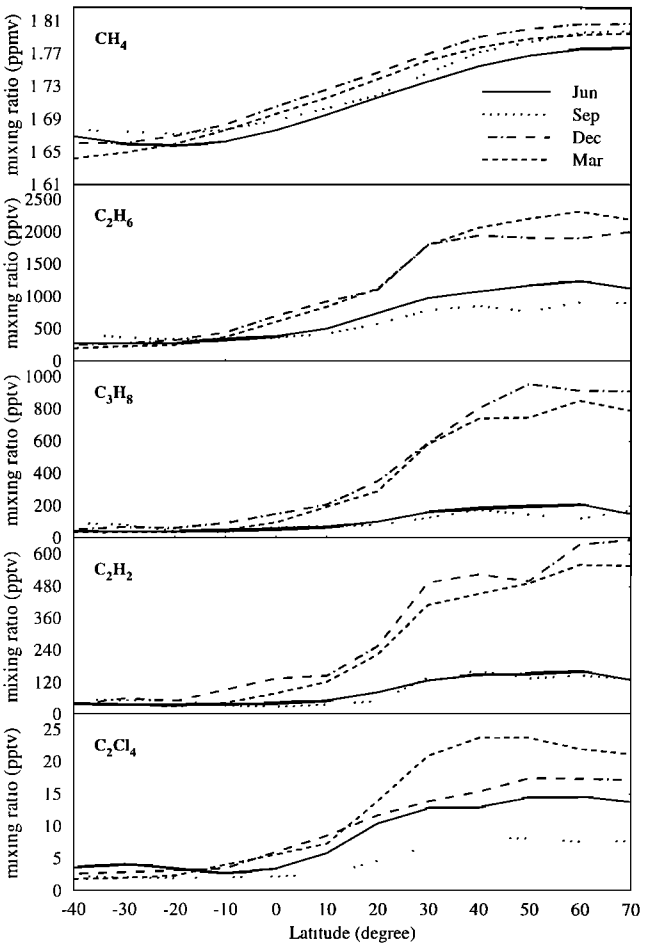

Figure 1. Seasonal variations in interpolated latitudinal distribution of surface mixing ratios of CH_4 (averaged for 1988–1991), C_2H_6, C_3H_8, C_2H_2 (averaged for 1989–1991), and C_2Cl_4 (1989–1990) measured by the D. R. Blake and F. S. Rowland group at UCI.

tainties in the source strengths of NMHCs, assessing the behavior of their oxidation byproducts such as organic nitrates, etc., which play important roles in tropospheric photochemistry, is also very difficult. Among all the NMHCs, only ethane, the longest-lived and the most abundant saturated NMHC, displays a significant increasing tropospheric burden [*Ehhalt et al.*, 1991].

In this paper, we calculate the annual global surface source strengths of relatively long-lived C_2H_6, C_2H_2, and C_3H_8 and their corresponding latitudinal distributions. In addition to these light parent NMHCs, CH_4 and tetrachloroethene (C_2Cl_4), a mainly industrially produced chemical, have also been included in the present study to assess their tropospheric budgets. In steady state, in the absence of in situ atmospheric sources, for all these species the global surface source strengths can be equated to their corresponding total atmospheric photochemical losses. The fact that OH radicals are the main sink of surface-emitted light NMHCs and C_2Cl_4 (with more than 80% of their sources originating from the northern hemisphere (NH), as concluded in this paper) and because industrial sources of C_2Cl_4 are seasonally independent [*McCulloch and Midgley*, 1996], C_2Cl_4 is used to examine the seasonal changes in the surface source strengths of C_2H_6, C_2H_2, and C_3H_8. To approach these objectives, we have used the seasonally varying surface concentration measurements of these hydrocarbons and C_2Cl_4 (described in section 2) as their lower boundary conditions in a two-dimensional global photochemical model. A brief description of this model is given in section 3. For this purpose, we have developed two photochemical schemes PC1 and PC3 which contain CH_4 and CH_4, C_2H_6, C_2H_2, C_2H_4, C_3H_8, and C_3H_6 as parent hydrocarbons, respectively. Details of these schemes are given in section 4. Features and dependence of OH radical distributions calculated using these schemes are described in section 5. Results and discussions of computed global source strengths for C_2H_6, C_2H_2, C_3H_8, and C_2Cl_4, including CH_4, and seasonal variations in surface sources of light NMHCs are given in sections 6 and 7, respectively. Finally, section 8 summarizes the major findings of this paper.

2. Surface Measurements of Light Hydrocarbons and C_2Cl_4

One of the goals of this paper is to estimate surface source strengths of light hydrocarbons and C_2Cl_4. Surface emission estimates of CH_4 from various sources are reasonably well constrained within a certain range [*Cicerone and Oremland*, 1988; *Crutzen*, 1991], but for NMHCs, as stated earlier, there still exist many uncertainties in the identities, and hence in the magnitudes of their source strengths. With the exception of CH_4 which also has soil sinks (about 6% of its total global sink [*Cicerone and Oremland*, 1988; *WMO*, 1994]), all the listed hydrocarbons and C_2Cl_4 included in this study have their surface emissions balanced by corresponding atmospheric chemical losses primarily by OH radicals. For some species, reactions with O_3, NO_3, and Cl radicals are other minor sinks. The characteristic that in steady state, global atmospheric chemical removals of hydrocarbons and C_2Cl_4 are equal to their total surface sources has made it possible to interactively calculate their surface emissions using a photochemical model and their corresponding surface measurements.

To accomplish this, we used surface observation data for the listed hydrocarbons and C_2Cl_4 collected during University of California, Irvine's (UCI's) trace gas program [*Smith*, 1993; *Wang et al.*, 1995]. Under this program, air samples were collected each season along the Pacific rim over a wide latitude range from 71°N to 47°S. To avoid the possible calibration differences among various working groups around the world [*Apel et al.*, 1994], no effort is made to combine their data with UCI's observations. The use of data from a single investigator is required to allow the self-consistent deduction of latitude gradients of surface sources. For CH_4, seasonally varying data averaged over four successive years (1988–1991) and for NMHCs and C_2Cl_4, data for (1989–1991) and (1989–1990), respectively, were used. Before treating the raw data over these periods, data corresponding to contamination and pollution events were removed. All observation data collected at the same latitude for different days of the same season were averaged. For each model grid location, these averaged data were spatially interpolated using the running average technique. For the model latitudes that lie outside the domain 71°N–47°S for which no observations exist, we assumed the same concentration as for the nearest available latitude. After averaging over the same seasons (which is applicable only for hydrocarbons), all these points were linearly interpolated on 1 day time resolution. Figure 1 shows the resultant seasonally and latitudinally varying treated surface mixing ratios of CH_4,

C_2H_6, C_2H_2, C_3H_8, and C_2Cl_4. Annually averaged observed mixing ratios at the surface for these species are 1.75 ppm (CH_4), 1150 ppt (C_2H_6), 330 ppt (C_3H_8), 230 ppt (C_2H_2), and 12 ppt (C_2Cl_4) for the NH and 1.67 ppm (CH_4), 310 ppt (C_2H_6), 50 ppt (C_3H_8), 40 ppt (C_2H_2), and 3 ppt (C_2Cl_4) for the southern hemisphere (SH). In general, all species show significant seasonal and latitudinal variations (see Figure 1) that are governed by their diverse spatially and temporally varying source distributions combined with their variable atmospheric lifetimes and interhemispheric exchange transport. For further discussion of these measurements and corresponding analysis and interpretation, refer to the references cited in this section.

3. Model Description

For the present study, we used a modified version of the Oslo two-dimensional (altitude-latitude) global tropospheric photochemical model [*Gupta*, 1996]. The original version of this model was developed by *Isaksen and Rodhe* [1978]. In the modified model the vertical domain has been increased by 8 km. In the vertical direction the model extends from the surface to 24.5 km with a total of 49 vertical layers and uniform resolution of 0.5 km. In latitude the model resolution is 10°. The main purpose of extending the model domain is to isolate the dependence of atmospheric distributions of light NMHCs from their upper boundary condition and to better simulate their photochemistry in the upper troposphere. By making this change the rigidity of the upper boundary condition can be relaxed because of the combined fast removal of these NMHCs by Cl and OH radicals in the upper troposphere and lower stratosphere [*Chameides and Cicerone*, 1978; *Singh and Kasting*, 1988].

The advective and diffusive transport coefficients for the modified model are those derived from the Geophysical Fluid Dynamics Laboratory general circulation model (GFDL GCM) [*Plumb and Mahlman*, 1987]. The transport features of this model have been tested with observed distributions and trends of CFC-11, CFC-12 [*Cunnold et al.*, 1994], and ^{85}Kr [*Weiss et al.*, 1983] tracers yielding an interhemispheric exchange time of about 1 year [*Gupta*, 1996]. This model has been used to simulate the global distribution of $\delta^{13}CH_4$ and its dependence on kinetic isotopic fractionations associated with various sinks of CH_4 [*Gupta et al.*, 1996, 1997].

Another modification made to the Oslo model is the inclusion of parameterized treatment for convective or subgrid scale vertical transport. This transport process is very important for the short-lived species which have chemical lifetimes of the order of a few days to weeks. Through this process, a polluted air mass containing a mixture of nitrogen oxides and hydrocarbons and CO, in addition to other pollutants, can be transported upward from the planetary boundary layer (PBL) to the free troposphere where the chemistry of these pollutants very efficiently forms O_3 molecules and hence significantly affects its distribution [*Lelieveld and Crutzen*, 1994]. Changing the distribution of O_3 in the upper troposphere and lower stratosphere can be very important radiatively [*Lacis et al.*, 1990]. In this model the treatment for fast vertical transport by convective clouds and frontal circulation due to cyclones at midlatitudes is based on the parameterization scheme developed by *Langner et al.* [1990]. For both of these fast vertical transports the model draws air out of the PBL (considered to be the first two model layers) at a specified rate depending upon the latitude and season. The boundary layer air is then detrained into the remaining part of the troposphere above the boundary layer according to a specified detrainment vertical profile which is also a function of latitude and season. For each latitude the mass continuity is maintained by compensating subsidence in the respective vertical column. For convective cloud transport this formulation is similar to the one developed by *Chatfield and Crutzen* [1984]. This approach is believed to capture the most important features of the convective transport mechanism for atmospheric species with a source in the boundary layer and has been applied to simulate the distributions for SO_2 and ^{222}Rn [*Langner et al.*, 1990]. For the modified model the seasonal and latitudinal distributions of mass fluxes due to cloud convection and midlatitude frontal cyclones and their respective vertical detrainment profiles are adopted from *Langner et al.* [1990].

4. Development of Photochemical Modules

In addition to the transport processes, sources and sinks of various chemical species and their mutual chemical interactions define the behavior of atmospheric pollutants. These pollutants may originate either from their surface emissions (natural and/or anthropogenic) or in situ production, or a combination of both. Various gas- and liquid-phase reactions and heterogeneous losses due to deposition at the Earth's surface, on aerosols, and rain droplets account for the ultimate fate of atmospheric pollutants. The following subsections briefly describe these points including the details about the photochemical schemes PC1 and PC3.

4.1. Emissions and Boundary Conditions

For the parent hydrocarbons, depending upon the purpose of the model simulation, two different types of lower boundary conditions were employed. For the deduction of surface emission strengths of light hydrocarbons and C_2Cl_4, their observed surface concentrations were used as the lower boundary condition. To investigate the seasonality in their sources, the calculated annual latitudinal surface emissions were uniformly applied on per time step basis at the lower boundary. For acetone, also a byproduct of C_3 or higher hydrocarbon oxidation, a surface emission strength of 25 Tg/yr due to biomass burning and biogenic emissions, as concluded by *Singh et al.* [1994], was equally distributed on per time step basis primarily at tropical latitudes. For C_2H_4 and C_3H_6 their seasonally varying observed surface mixing ratios averaged for (1989–1991), as described in section 2, were used as the lower boundary condition. At the upper boundary, CH_4 was allowed to diffuse through the top of the model according to the one-dimensional vertical steady state scale height approximation using its losses against OH and Cl radicals in the stratosphere. For NMHCs and C_2Cl_4, mixing ratios just above the model domain were fixed as 0.25 times that at the topmost layer; that is, $\chi_{50} = f \times \chi_{49}$, where χ is the mixing ratio and f is equal to 0.25. This upper boundary condition for NMHCs is relatively rigid but is appropriate because by 25 km, their concentrations decrease very rapidly with altitude [*Rudolph et al.*, 1981, 1984], thereby making their atmospheric distributions completely independent of upper boundary conditions. In fact, simulations performed with variable value of f ranging between 0 and 1 showed no difference in the vertical profiles of these species [*Gupta*, 1996].

Annual source strengths of NO_x, HNO_3, O_3, and CO used in

Table 1. Annual Source Strengths of CO, O_3, NO_x, HNO_3, and Acetone Used in the Model Calculations

Species	Source Strength
NO_x, Tg N/yr	
Surface	37
Lightning	8
Aircraft	0.67
Stratosphere	0.45
HNO_3 stratospheric source, Tg N/yr	0.66
O_3 stratospheric source, Tg O_3/yr	656
CO surface source, Tg CO/yr	1280
Acetone, Tg CH_3COCH_3/yr	25

With the exception for acetone, all other emission strengths listed in this table are adopted from *Isaksen and Hov* [1987] and *Fuglestvedt et al.* [1993]. For acetone the annual source strength estimate is taken from *Singh et al.* [1994].

present model simulations are summarized in Table 1. The surface source estimates and NO_x emissions from aircraft and lightning listed in this table with their corresponding latitudinal distributions were adopted from *Isaksen and Hov* [1987] and *Fuglestvedt et al.* [1993]. For NO_x and CO, north to south surface emission ratios are 4.2 and 2.6, respectively. For both of these species the surface emissions were applied equally on per time step basis. Stratospheric subsidence rates of O_3, NO, and HNO_3 and their corresponding latitudinal and seasonal distributions were taken from the Oslo two-dimensional tropospheric-stratospheric model [*Stordal et al.*, 1985; *Isaksen and Stordal*, 1986].

For all simulations, full interactive photochemical calculations with transport were performed for the model region between surface and 16.5 km. The extended region of the model between 16.5 and 24.5 km was only used for the transport of light hydrocarbons and C_2Cl_4 and for their chemical losses due to prescribed distributions of OH and Cl radicals. Monthly averaged distributions of Cl and OH radicals for the extended region were taken from the Oslo two-dimensional tropospheric-stratospheric model. Also, for the marine boundary layer (MBL), monthly varying distributions of Cl radicals were adopted from the Oslo model. In this model the only source of chlorine radicals in the MBL is due to reaction of HCl with OH radicals. The concentrations of Cl radicals in the MBL and atmospheric region of (16.5–24.5) km are of the order of (5×10^2–4×10^3) and (7×10^3–4×10^4) molecules cm^{-3}, respectively. Monthly varying two-dimensional water vapor distributions were adopted from *Barnett and Corney* [1985].

Dry deposition loss frequencies for O_3, NO_2, H_2O_2, HNO_3, and PAN were calculated for the lowest layer in terms of their corresponding deposition velocity given at 1 m [*Isaksen and Rodhe*, 1978]. These loss frequencies were weighted by the land and oceanic areas per 10° latitude band. Also, the seasonal dependence of land surface deposition velocity was also incorporated as mentioned by *Isaksen et al.* [1985]. Table 2 lists the deposition velocities of various species used in the model calculations. To examine the effects of the CO soil sink, the deposition velocity corresponding to this loss is also given in Table 2.

4.2. Photochemical Schemes

Two photochemical schemes, PC1 and PC3, were developed for the present study which focus on the fate of six light parent hydrocarbons, namely CH_4, (C_2H_6, C_2H_4, C_2H_2) and (C_3H_8, C_3H_6) and their oxidation byproducts. Photochemical scheme PC1 contains only CH_4, while in addition to CH_4, scheme PC3 also includes C_2 and C_3 compounds. Tetrachloroethene is included in both of these schemes. Initially, we adopted the PC1 chemical scheme from *Isaksen and Hov* [1987] and modified it to include some reactions of oxidation byproducts such as methyl alcohol, formic acid, nitrous acid, etc. The rate constants of this scheme were updated using the recommendations of *Atkinson et al.* [1992] and *DeMore et al.* [1992]. Presently, the chemical scheme PC1 has about 150 thermal and photolytic reactions involving 45 species. Inclusion of complex and extensively branched chemistry of C_2 and C_3 parent hydrocarbons and their byproducts increased the total number of reactions to about 750 involving more than 200 species [*Gupta*, 1996]. Some reactions of parent hydrocarbons and their byproducts involving Cl radicals in the MBL, upper troposphere, and lower stratosphere were also included. For both schemes, rate constants of primary reactions of parent hydrocarbons and C_2Cl_4 were updated from *DeMore et al.* [1997], *Kaiser and Wellington* [1996], and *Atkinson* [1994].

Photodissociation rates for all species of both photochemical schemes were calculated according to the two-stream approximation method developed by *Isaksen et al.* [1977] and modified by *Jonson and Isaksen* [1991] to account for diffuse radiation by Rayleigh and Mie scattering due to cloud droplets and aerosol particles. The data for actinic solar flux and absorption cross sections and quantum yields of all the species undergoing photodissociation were taken from *DeMore et al.* [1985, 1992]. For the middle of each month, all photodissociation rates were calculated off-line at 15 min time and 10° latitude intervals, with and without cloud cover. Both sets of these photodissociation rates (with and without cloud cover) were averaged over 1 hour time intervals for their later use in diurnal photochemical calculations.

The chemical part of the two-dimensional model equation was solved using the time-flux operator splitting method and "quasi steady state approximation (QSSA)" [*Hesstvedt et al.*, 1978]. To maximize mass conservation and to use longer time steps for integration, the chemical family technique was used in addition to constraining the sum of concentrations of rapidly cycling species such as OH/HO_2, HO_2/HO_2NO_2, and NO/NO_2 [*Berntsen and Isaksen*, 1994]. For all the simulations, typically the model was allowed to run for at least 4 decades to ensure the attainment of steady state concentrations of CH_4 in the entire model domain. More details about photochemical schemes, calculation of photorates, and diurnal averaging and their use for the solution of long-lived species are given by *Gupta* [1996].

Table 2. One Meter Deposition Velocity of Various Species for Land and Oceanic Surfaces Used in the Model Calculations

Species	Land	Ocean
O_3	0.5	0.1
NO_2	0.2	0.2
HNO_3	1.0	1.0
PAN	0.2	0.2
CO	0.03	0.0
H_2O_2	1.0	1.0

All these deposition velocity values (cm s^{-1}) are adopted from *Isaksen et al.* [1985] and *Berntsen and Isaksen* [1994].

4.3. CH_4 Perturbation Study

Photochemical schemes PC1 and PC3 with seasonally and latitudinally varying observed mixing ratios of light hydrocarbons, fixed CH_4 mixing ratio of 1.75 ppm for all seasons, and latitudes and annual emissions of other species as listed in Table 1 were used to perform the experiment named "delta-CH_4." This experiment was designed by IPCC working group I to evaluate the indirect effects of a 20% increase in CH_4 concentration on the tropospheric O_3 and NO_x distributions and on OH concentrations. Following the protocol for this experiment (M. J. Prather, personal communication, 1996), we also determined the ratio of adjustment time to steady state lifetime [*Gupta*, 1996]. For both photochemical schemes PC1 and PC3 the calculated ratios were 1.43 and 1.39, respectively, which are in good agreement with estimate of 1.45 ± 0.25 reported by *IPCC* [1994]. The value of this ratio was also verified by direct adjustment time calculation for perturbation simulation. The adjustment time for a CH_4 pulse perturbation to scheme PC1 was found to be 14 years, which when divided by its steady state lifetime of 9.72 years yielded 1.44 as the ratio of adjustment time to steady state lifetime.

5. Computation of Hydroxyl Radical Distribution

The hydroxyl radical is central to tropospheric photochemistry. Despite its low concentration (of the order of 10^5–10^6 molecules cm^{-3}), it is a principal sink for numerous atmospheric pollutants. Global spatial and temporal distributions of OH radical can be calculated using photochemical models [*Chameides and Tan*, 1981; *Crutzen and Zimmermann*, 1991; *Spivakovsky et al.*, 1990]. The OH distributions calculated in this way can be validated by simulating the observed surface methyl chloroform distributions and their trends [*Spivakovsky et al.*, 1990; *Taylor et al.*, 1991; *Tie et al.*, 1992].

In the present study, we have photochemically derived the OH distribution using the observed surface distributions of light hydrocarbons as their lower boundary condition. Emission strengths of all species other than hydrocarbons used in these calculations are shown in Table 1. For scheme PC1 the calculated diurnal variation of OH radical concentration is a strong function of altitude as shown in Figure 2 for July at 40°N and at 0.25, 6.25, and 15.25 km. At low altitudes, daytime OH concentrations are only 40–80 times higher than the corresponding nighttime values. We attribute this feature to the rapid recycling of HO_2 radicals due to HO_2NO_2 and O_3 molecules by the following sequence of reactions: During the nighttime the main source of HO_2 radicals is the unimolecular decomposition of HO_2NO_2:

$$HO_2NO_2 + M \rightarrow HO_2 + NO_2 + M$$

The NO_2 formed in this reaction is oxidized to form NO_3 which is responsible for a significant amount of nighttime oxidation chemistry. These species recombine to form N_2O_5. Similar to daytime, the reaction of HO_2 with O_3 produces OH radicals during the nighttime:

$$HO_2 + O_3 \rightarrow OH + 2O_2$$

The hydroxyl radicals formed during the night regenerate HO_2 radicals from their reaction with CO:

$$CO + OH + O_2 \rightarrow HO_2 + CO_2$$

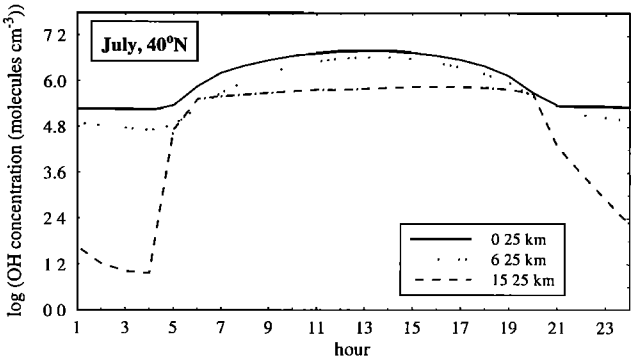

Figure 2. Diurnal variations in OH concentration for July at 40°N and at 0.25, 6.25, and 15.25 km calculated using photochemical scheme PC1. Our model calculates larger nighttime OH values near the surface than earlier models, but the effect of these nighttime values on 24-hour average values is negligible.

In the polluted boundary layer, nighttime emissions of NO can also form OH radicals:

$$HO_2 + NO \rightarrow OH + NO_2$$

The NO_2 formed in this reaction recombines with HO_2 to form HO_2NO_2. Also, owing to the low concentrations of HO_2 and OH radicals during the night, the time constants of the decay of HO_x species from (HO_2 + HO_2) and (HO_2 + OH) reactions, which account for the net loss of HO_x species, are relatively higher (approximately by 2 orders of magnitude in the lower troposphere) compared to the corresponding values during the daytime. Very low nighttime OH concentrations at high altitudes is due to low HO_2 concentrations. For the lower troposphere this feature in diurnal variation has been reported by *Lu and Khalil* [1991] and *Bey et al.* [1997]. On the basis of nighttime measurement of HO_2 of about 10 ppt during night at 48°N, *Mihelcic et al.* [1993] estimated the nighttime OH concentration of 10^5 molecules cm^{-3}, which is in accordance with the analysis of *Platt et al.* [1990]. Recently, *Tanner and Eisele* [1995] reported nighttime OH concentration measurements in the range of 10^4 molecules cm^{-3} using ion-assisted technique.

Figure 3 shows the diurnally averaged OH distributions for the months of July and January. During the summer of both hemispheres the maximum concentration is observed around 25° which is consistent with other model studies [*Crutzen*, 1987; *Spivakovsky et al.*, 1990]. This seasonal variation in OH distribution is mainly due to seasonality in the solar UV flux reaching the troposphere which is responsible for the OH production through the photodissociation of O_3 molecules followed by the reaction $O(^1D)$ + H_2O. Generally, OH radical number densities decrease with altitudes, but in the upper troposphere and lower stratosphere a slight increase in OH density is calculated. This pattern in vertical profile of OH radicals is consistent with that of *Tie et al.* [1992] but differs from that of *Spivakovsky et al.* [1990]. Despite the decrease in water vapor concentration in upper troposphere and lower stratosphere, the increase in O_3 concentration and its photolysis rate cause this increase in OH concentration. The monthly averaged OH concentration for each hemisphere (weighted by distributions of rate constant for reaction CH_4 + OH and CH_4 concentration [*Prather and Spivakovsky*, 1990]) shows the maximum value in summer (1.3×10^6 cm^{-3} and 1.4×10^6 cm^{-3} for NH

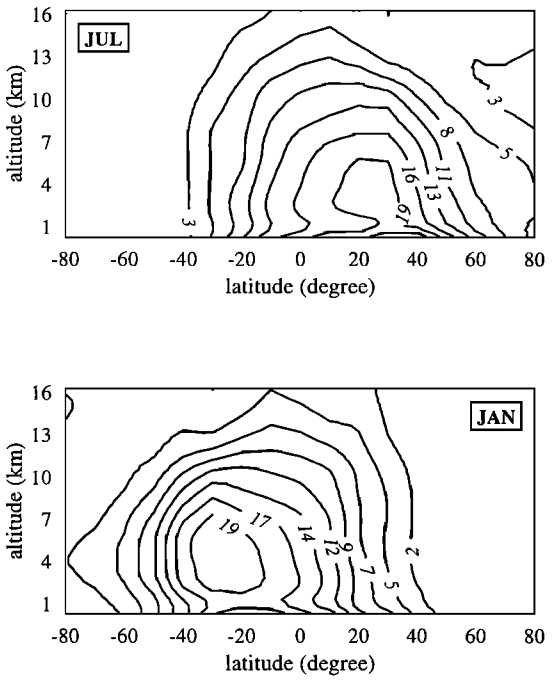

Figure 3. Global distributions of diurnally averaged OH concentrations ($\times 10^5$ molecules cm^{-3}) for July and January calculated using photochemical scheme PC1.

and SH, respectively) and the minimum (6.6×10^5 cm^{-3} and 7.4×10^5 cm^{-3} for NH and SH, respectively) in winter. Peak-to-peak ratio of hemispherically averaged OH concentration over a year is found to be higher in the SH (2.2) as compared to that in the NH (2.1). Globally averaged OH radical concentration derived from scheme PC1 is 1.03×10^6 molecules cm^{-3}. On the annual average basis the north to south hemispheric OH concentration ratio is 0.89 because of the higher OH concentration in the SH. This result is consistent with other modeling studies [*Chameides and Tan*, 1981; *Crutzen and Gidel*, 1983; *Tie et al.*, 1992] and observations [*Brenninkmeijer et al.*, 1992] but disagrees with the results of *Spivakovsky et al.* [1990].

For the termolecular reaction of OH and NO_2 leading to formation of HNO_3, we used the rate constant recommended by *Atkinson et al.* [1992]. New rate measurements for this reaction reported by *Donahue et al.* [1997] indicate that at 300 K and for pressure region 20–600 torr, the rate constant may be higher by 10–30%. It remains, however, to determine whether this correction applies to all tropospheric temperatures. If so, the revised rate constant will lead to an increase in OH concentration in comparison with that calculated here. There are two primary reasons for this speculation: lowering the OH radical loss rate due to the stated reaction and increase in O_3 formation due to more availability of NO_2 radicals to photolyze.

5.1. Effect of Convective Transport

As mentioned before, vertical convection draws polluted air from the boundary layer which has enhanced concentrations of CO, hydrocarbons, NO_x, and HNO_3 and returns the upper tropospheric air which is rich in O_3. Simulating this fast exchange of air makes tropospheric chemistry more complex and augments the oxidizing capacity of the troposphere by increasing overall OH concentration, as shown in Figure 4. This figure illustrates the percent change in OH concentration for the month of July from convection. In the lower troposphere this increase is as much as 5%, and for the upper tropical troposphere it ranges from 15% to more than 45%. On an annual basis, compared to the nonconvective PC1 case, the global average OH concentration increased by 3%. In the lower troposphere this increase is due to more O_3, whose photolysis forms $O(^1D)$ and hence more OH radicals. Another important effect of convective transport on tropospheric chemistry is to increase the O_3 formation efficiency per NO molecule consumed. For given NO emissions the increase in O_3 formation efficiency per NO molecule in the PBL is due to decreased background NO concentrations caused by convective dilution [*Liu et al.*, 1987]. Decreases in concentrations of CO and CH_4 resulting from dilution of the PBL layer also increased OH concentrations. In the upper troposphere the relatively enhanced oxidation of CO and CH_4 in the NO-rich environment increased the production of OH radicals.

5.2. Effect of Addition of C_2 and C_3 Parent NMHCs

Addition of C_2 and C_3 parent hydrocarbon oxidation has significant effects on regional OH concentrations, but little effect on global annually averaged OH concentration. In the lower troposphere at higher latitudes, diurnally averaged OH concentrations derived from scheme PC3 are decreased by as much as 10% relative to that from scheme PC1, as shown for July in Figure 5. However, in the northern hemispheric upper troposphere during summer, OH concentration is increased by more than 8% due to higher NO_x concentrations (from oxidation of organic nitrates) which caused increased oxidation of hydrocarbons and hence enhanced production of O_3 and OH radicals [*Crutzen*, 1987]. Also for this region, the OH removal

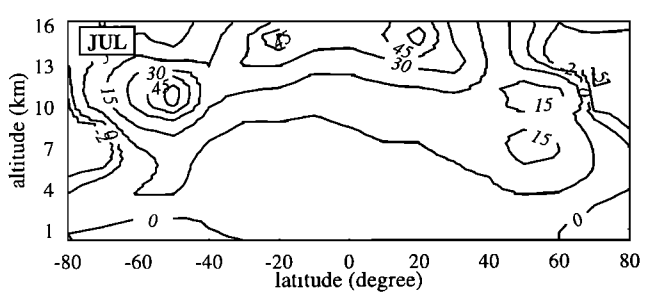

Figure 4. Calculated percent changes in diurnally averaged OH concentration for the month of July due to inclusion of convective transport to photochemical scheme PC1.

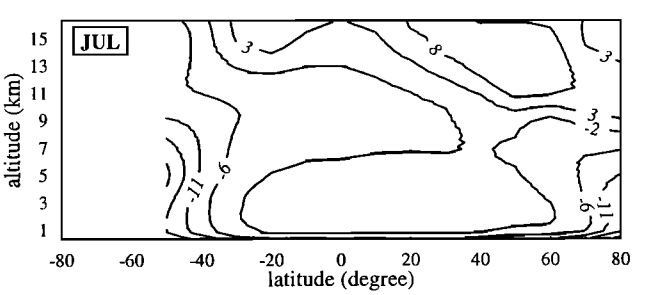

Figure 5. Calculated percent changes in diurnally averaged OH concentration for July due to inclusion of photochemistry of C_2 and C_3 light hydrocarbons to scheme PC1.

rate is small due to the negligible rainout probability of HNO_3, a major sink of OH in the lower troposphere. Overall, the global averaged OH concentration is decreased by 2%. Also, for scheme PC3 the calculated interhemispheric north to south OH concentration ratio decreased slightly (to 0.888 as compared to 0.893) from scheme PC1 because of higher northern hemispheric concentrations of C_2 and C_3 parent hydrocarbons and their oxidation byproducts.

5.3. Effect of Soil Sinks of CO and CH_4

Inclusion of soil sinks of CH_4 and CO to photochemical scheme PC1 has a significant effect on global and hemispheric OH distributions. For the CO soil sink a surface deposition velocity of 0.03 cm/s was used [*Seiler and Conrad*, 1987; *Hough*, 1991] which is higher than the 0.02 cm/s used by *Crutzen and Zimmermann* [1991]. In steady state the calculated magnitude of this soil sink for CO is 278 Tg/yr which is comparable to the lower limit (250 Tg/yr) recommended by *WMO* [1994]. *Pinto et al.* [1983] used 0.04 cm/s for the CO deposition velocity and calculated a corresponding sink of 480 Tg/yr. For CH_4 we used a constant soil sink of 30 Tg/yr [*WMO*, 1994], which is distributed proportionally to the land surface area. For July, inclusion of both sinks increased diurnally averaged OH concentrations by as much as 8% at higher northern hemispheric altitudes. At lower altitudes this increase is relatively smaller as shown in Figure 6. On the global average basis the hydroxyl radical concentration increased by 2%, and the interhemispheric ratio increased to 0.91 as compared to the corresponding values of 0.89, respectively, derived without the soil sink and scheme PC1.

5.4. Test of Validation Using Methyl Chloroform

The hydroxyl radical distribution calculated interactively with photochemistry was validated by simulating the latest reported observed trend and surface distributions of methyl chloroform (MCF) [*Prinn et al.*, 1995]. Like CFC-11 and CFC-12, MCF is also solely of anthropogenic origin. It is mainly destroyed by OH radicals in the troposphere, while oceans and stratospheric photolysis are two minor sinks. Thus MCF serves as an indicator for tropospheric OH concentrations. Using the industrial emission inventories of MCF for 1951–1991 and their latitudinal fractions as reported by *Prinn et al.* [1987, 1995] and *Fisher et al.* [1994], its atmospheric distributions and trends have been simulated [*Gupta*, 1996]. The model calculated an instantaneous global lifetime of MCF for 1991 of 5.2 years which is 7.5% higher than the Atmospheric Lifetime Experiment/Global Atmospheric Gases Experiment (ALE/GAGE) estimates [*Prinn et al.*, 1995]. The global averaged lower atmospheric (1000–200 mbar) lifetime of MCF for 1991 was 4.6 years which is exactly that reported by *Prinn et al.* [1995]. Similar to observed trends [*Prinn et al.*, 1995], the model calculated a 2.5% MCF concentration decrease for northern hemispheric latitudes for the period December 1990 to December 1991.

6. Global Distributions and Source Strengths of Light Hydrocarbons and Tetrachloroethene

6.1. Light Hydrocarbons

Into the atmosphere a large number of NMHCs are emitted from natural and anthropogenic sources. The sum of total emissions of all NMHCs exceeds that of CH_4 sources. Biomass burning, natural gas emissions, incomplete combustion, ocean,

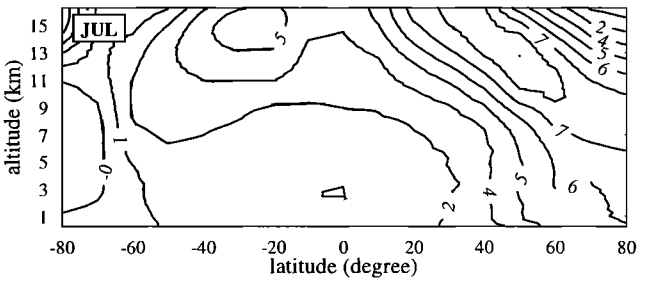

Figure 6. Calculated percent changes in diurnally averaged OH concentration for the month of July due to inclusion of soil sinks of CO and CH_4 to photochemical scheme PC1.

and vegetation are thought to be the main sources of NMHCs. Compared to CH_4, at room temperature, chemical reactivities of C_2H_6 and C_3H_8 are about 40 and 170 times faster toward OH radicals, and about 550 and 1330 times faster toward Cl radicals. Therefore these species are relatively short-lived.

Study of the global distributions of parent NMHCs and their oxidation byproducts requires knowledge of their surface sources. Several regional sources and their strengths for individual and/or combined hydrocarbons have been reported [*Brice and Derwent*, 1978; *Nelson et al.*, 1983; *Tille et al.*, 1985; *Lamb et al.*, 1987; *Kanakidou et al.*, 1989; *Field et al.*, 1992], but their global extrapolation is uncertain because of geographically varying industrial and natural activities. Also, global emissions of all NMHCs (classified into different categories such as paraffins, olefins, aromatics, and terpenes) in terms of total carbon content have been estimated [*Duce et al.*, 1983; *Piccot et al.*, 1992; *Fehsenfeld et al.*, 1992; *Müller*, 1992; *Guenther et al.*, 1995]. There are some estimates available for the global source strength of individual light hydrocarbons [*Penkett*, 1982; *Isaksen et al.*, 1985; *Ehhalt et al.*, 1986; *Blake and Rowland*, 1986; *Kanakidou et al.*, 1991a, b; *Roemer and van den Hout*, 1991; *Hough*, 1991; *Singh and Zimmerman*, 1992; *Strand and Hov*, 1994; *Rudolph*, 1995], but these individual estimates for particular species cover a large range. For example, annual global surface source strength of C_2H_6 from these estimates ranges from 5 to 52 Tg (1 Tg = 10^{12} g) (see Table 4). Because of the lack of understanding of types and strengths of various sources of individual hydrocarbons, we have calculated the total surface source strengths of C_2H_6, C_2H_2, and C_3H_8 using their seasonally and latitudinally varying observed surface mixing ratios, as described in section 2, and OH radical distribution derived from scheme PC3 and validated by methyl chloroform simulations. In addition, we have also calculated annual surface source strengths of CH_4 and C_2Cl_4.

At the end of each 1 day time step our calculated surface mixing ratios of the stated species at all latitudes were replaced by the corresponding interpolated observed values of the next day. In steady state the cumulative annual difference between the calculated and updated observed surface mixing ratios at all latitudes for each species was translated into a global source strength. For these initial calculations the convective transport process was not included. Computed steady state annual surface emissions of these hydrocarbons, corresponding north to south ratios of their annual source strengths, and global lifetimes are given in Table 3. Among these NMHCs, C_2H_6 is the longest-lived with a global lifetime of 83 days.

Figures 7–9 show the latitude-time cross section of monthly surface removal rates (which are monthly integrated combined

Table 3. Global Source Strengths and Lifetimes of Light Hydrocarbons and C_2Cl_4 Calculated Using Nonconvective Photochemical Scheme PC3

Species	Source Strength, Tg/yr	North/South Source Ratio	Global Lifetime
CH_4	490 (500)	2.11	9.9 years
C_2H_6	10.35 (10.76)	4.02	83 days
C_3H_8	8.37 (8.70)	4.70	25 days
C_2H_2	3.14 (3.27)	3.97	32 days
C_2Cl_4	0.432 (0.448)	7.47	116 days

Numbers in parentheses correspond to simulation with convective transport.

losses due to chemistry and transport in the lowest model layer) of these NMHCs in steady state. For all three species the autumn season accounts for the maximum surface removal rate (more than 30% of the global annual removal rates). The calculated removal rates of these NMHCs at high latitudes represent their losses due to transport from other regions. The exact pattern of calculated removal rates depends on the model structure, for example, model resolution. Given the sparse spatial resolutions of surface measurements and geographical source distribution, our present use of model grid dimension is justifiable.

The latitude belt (30°N–60°N) accounts for more than 54% of the total annual global emissions of these NMHCs, and the latitude belt (20°N–20°S) accounts for more than 27% of their total annual global emissions. With lifetimes short compared to the model interhemispheric exchange time of about 1 year, the north to south surface source ratios of 4.0, 4.7, and 4.0 for C_2H_6, C_3H_8, and C_2H_2, respectively, indicate that 80% or more of their emissions occur in the NH. In steady state the total northern hemispheric annual sources are 8.3, 6.9, and 2.5 Tg for C_2H_6, C_3H_8, and C_2H_2, respectively, of which 1.1, 0.2, and 0.1 Tg, respectively, are transported to the SH where they are chemically destroyed. The maximum north to south interhemispheric flux for January of 0.2, 0.06, and 0.03 Tg for C_2H_6, C_3H_8, and C_2H_2, respectively, was calculated. Above 16.5 km, removal of C_2H_6 by chlorine dominates the total losses and causes a rapid decrease in its vertical mixing ratio; however, this loss of C_2H_6 by chlorine radicals is only 2% of its total global loss.

The calculated surface source strengths of these NMHCs and their comparison with other estimates are given in Table 4. For the given surface measurements the zonally averaged nature of our model and uncertainties in rate constants might cause some variations in our emission estimates. As mentioned before, inclusion of convective transport caused an increase in overall tropospheric oxidizing capacity which resulted in a net increase in annual source strength. For nonconvective and convective PC1 simulations the calculated global source strengths for C_2H_6 are 10.6 and 11.0 Tg/yr. For scheme PC3 these calculated values are 10.4 and 10.8 Tg/yr for the cases without and with the inclusion of convective transport. These estimates are in good agreement with the 10 Tg/yr estimate of *Isaksen et al.* [1985] and are within the 10–15 Tg/yr range reported by *Singh and Zimmerman* [1992]. Using surface observations, *Blake and Rowland* [1986] estimated 13 Tg/yr as the global source strength of C_2H_6. For C_2H_6, *Kanakidou et al.* [1991a] calculated the total emission of 16 Tg/yr and later modified it to 14 Tg/yr using a three-dimensional model [*Kanakidou et al.*, 1991b]. Recently, *Rudolph* [1995] estimated 15.5 Tg/yr emission strength for C_2H_6. The importance of chlorine-initiated oxidation of hydrocarbons has already been outlined by several studies [*Singh and Kasting*, 1988; *Finlayson-Pitts*, 1993; *Wingenter et al.*, 1996; *Keene et al.*, 1996]. Inclusion of chlorine removal of C_2H_6 throughout the troposphere increased the global emission to 13.3 Tg/yr calculated using the PC1 scheme without convection. In the lower troposphere, chlorine atom concentrations are in the range of 10^3 cm^{-3}. About 4–6 Tg/yr of the C_2H_6 global source strength has been

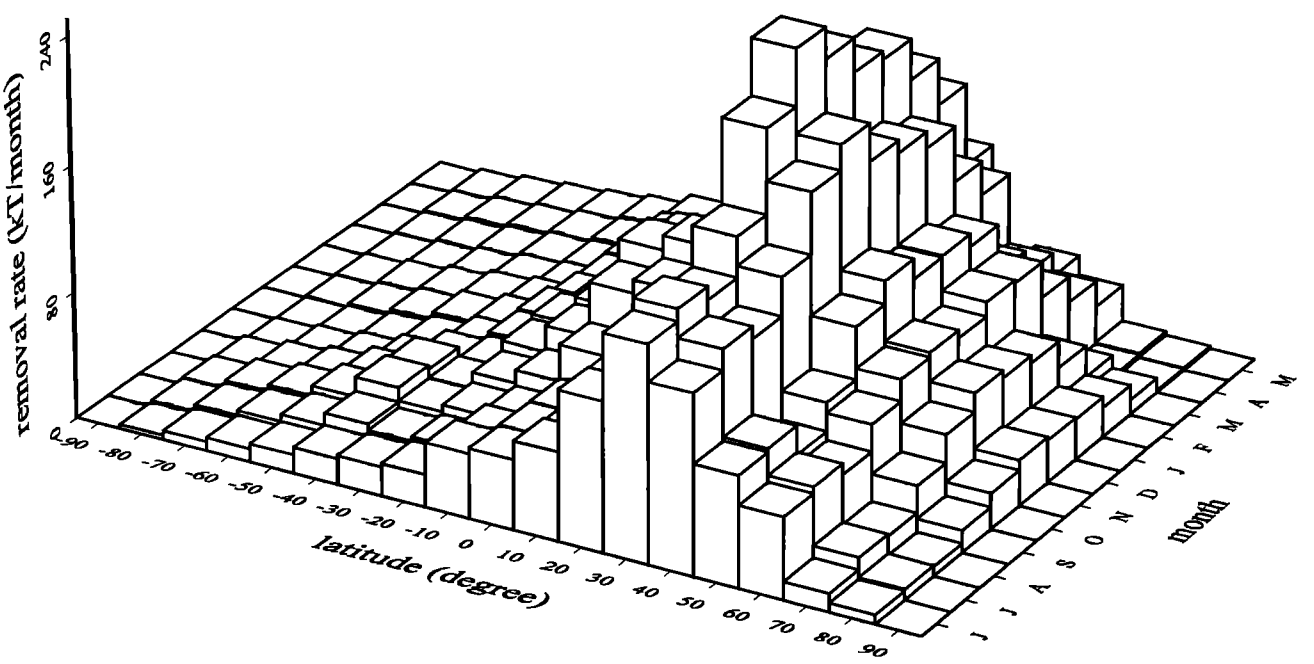

Figure 7. Latitude-time cross section of integrated monthly surface removal rates of C_2H_6 per 10° bin in steady state calculated using scheme PC3 and its surface observations.

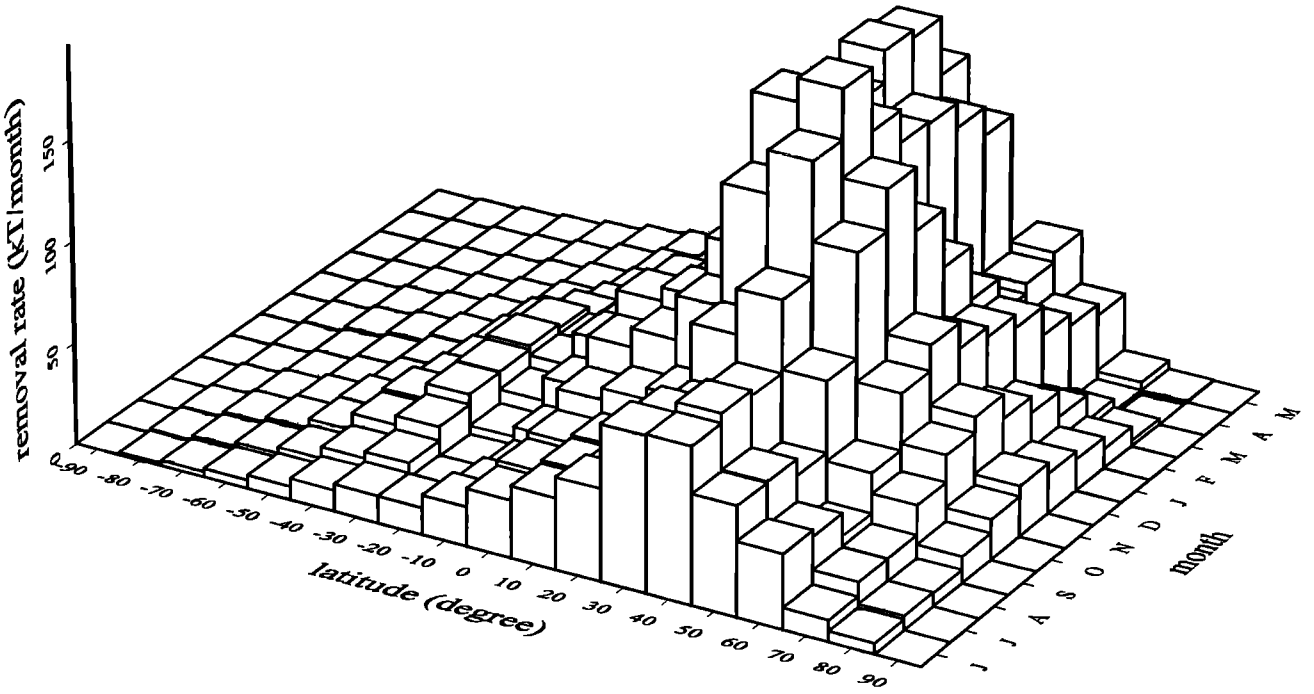

Figure 8. Latitude-time cross section of integrated monthly surface removal rates of C_3H_8 per 10° bin in steady state calculated using scheme PC3 and its surface observations.

assigned to biomass burning [*Ehhalt et al.*, 1986; *Singh and Zimmerman*, 1992; *Hegg et al.*, 1990; *Rudolph*, 1995; *N. J. Blake et al.*, 1996]. Ethane production from natural gas emission and oil combustion contributes about 2–6 Tg/yr to the total source [*Singh and Zimmerman*, 1992; *Rudolph*, 1995]. *Plass-Dulmer et al.* [1995] estimated oceanic C_2H_6 emission of 0.16 Tg/yr.

The steady state annual surface sources of C_3H_8 calculated using scheme PC3 without and with convective transport are 8.4 and 8.7 Tg, respectively, which are close to the estimates of *Isaksen et al.* [1985] but are lower than other reported estimates (see Table 4). Inclusion of chlorine removal of C_3H_8 in the troposphere increased its calculated emission from scheme PC1 (without convection) from 8.6 to 9.5 Tg/yr. Biomass burning (0.6–2.4 Tg/yr) [*Ehhalt et al.*, 1986; *Hegg et al.*, 1990; *N. J. Blake et al.*, 1996], natural gas emission (1–2 Tg/yr) [*Ehhalt et al.*, 1986; *Singh and Zimmerman*, 1992], and oceans (0.1–1.0

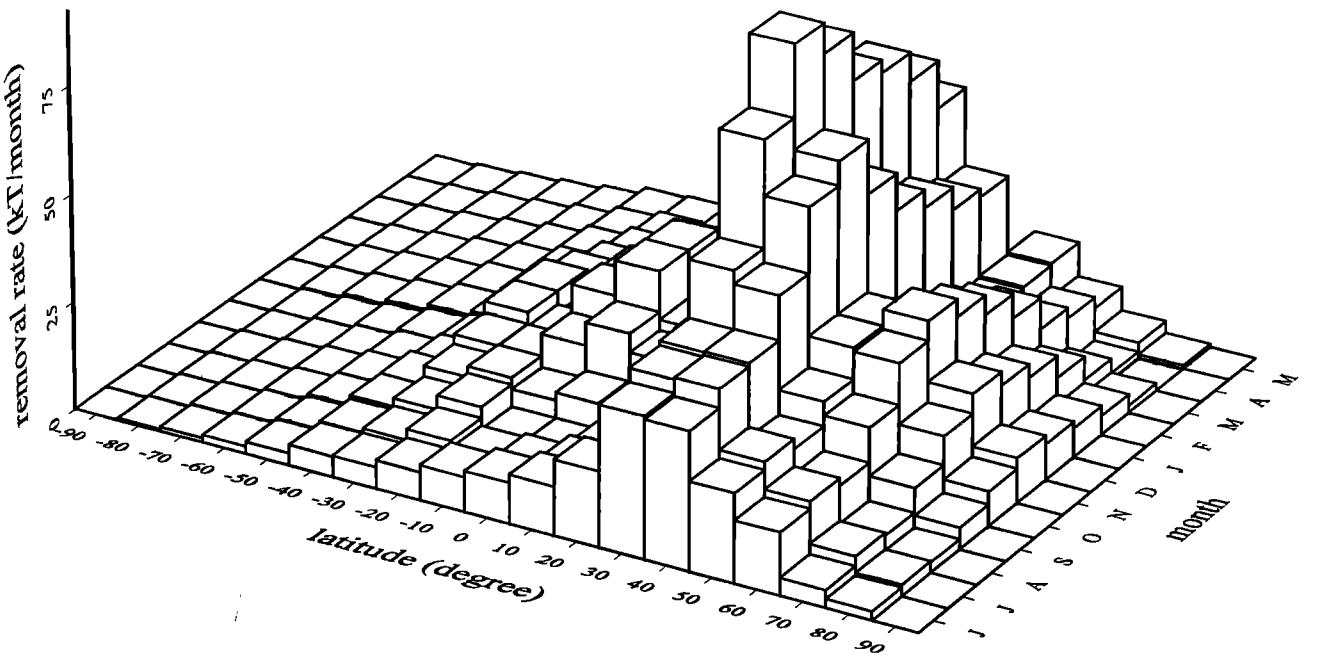

Figure 9. Latitude-time cross section of integrated monthly surface removal rates of C_2H_2 per 10° bin in steady state calculated using scheme PC3 and its surface observations.

Table 4. Comparison of Calculated Global Surface Source Strengths of Light NMHCs and C_2Cl_4 With Other Estimates

Reference	C_2H_6	C_3H_8	C_2H_2	C_2Cl_4
PC1A[a]	10.57	8.63	3.22	0.441
PC1B[b]	10.97	8.96	3.36	0.457
PC3A[c]	10.35	8.37	3.14	0.432
PC3B[d]	10.76	8.70	3.27	0.448
PC3C[e]	10.14	8.36	3.13	0.414
PC3D[f]				0.449
Ehhalt et al. [1986]	7.6	4.0	2.0	
Singh and Zimmerman [1992]	10–15	15–20	3–6	
Rudolph [1995]	15.5			
Kanakidou et al. [1991a]	16	23		
Kanakidou et al. [1991b]	14	17		
Blake and Rowland [1986]	13			
Isaksen et al. [1985]	10	10	2.7	
Roemer and Hout [1991]	15	25	5	
Fuglestvedt et al. [1993]	20	17		
Penkett [1982]	5			
Strand and Hov [1994]	52			
Hough [1991]	29	26.3	4.5	
Class and Ballschmitter [1986]				0.580
Wiedmann et al. [1994]				0.479
Koppmann et al. [1993]				0.580
Rudolph et al. [1996]				0.420
McCulloch and Midgley [1996]				0.423 ± 0.022 for 1989 0.366 ± 0.019 for 1990

All these source strengths are given in Tg/yr.

[a] Using scheme PC1 with chlorine removal between (16.5–24.5) km and without convection.

[b] Using scheme PC1 with chlorine removal between (16.5–24.5) km and with convection.

[c] Using scheme PC3 with chlorine removal between (16.5–24.5) km and without convection.

[d] Using scheme PC3 with chlorine removal between (16.5–24.5) km and with convection.

[e] Using scheme PC3 with no chlorine removal in entire model domain and without convection.

[f] Using scheme PC3 with chlorine removal in the lowest model layer and without convection.

Tg/yr) [*Plass-Dulmer et al.*, 1995; *Singh and Zimmerman*, 1992] are the main contributors to the total annual source of C_3H_8. Recently, *Blake and Rowland* [1995] suggested leakage from liquefied petroleum gas (LPG) as an important source of C_3H_8.

Our annual surface emission of C_2H_2 calculated using scheme PC3 is 3.1 Tg which increased to 3.3 Tg due to inclusion of convective transport. These estimates are close to those of *Singh and Zimmerman* [1992], *Ehhalt et al.* [1986], and *Isaksen et al.* [1985]. No significant effect on total computed source strength is observed when its removal by tropospheric chlorine is included. For example, for scheme PC1 the estimates of annual source strength for C_2H_2 with and without removal by Cl radicals in the troposphere are 3.23 and 3.22 Tg, respectively. Biomass burning [*Hegg et al.*, 1990; *N. J. Blake et al.*, 1996] and combustion are apparently the major sources of C_2H_2 [*Whitby and Altwicker*, 1978]. Oceanic emissions have also been suggested as a minor source of C_2H_2 [*Kanakidou et al.*, 1988; *Plass-Dulmer et al.*, 1995]. For all these light NMHCs and for all simulation cases, no difference was noted in the estimates of annual source strengths when their outgoing flux varied between two extremes, defined by *f* in section 4.1 at the upper boundary.

Figure 10 shows the steady state distributions of C_2H_6, C_3H_8, and C_2H_2 for the month of January. Significant presence of all these species is calculated in the model region above 10 km. In the southern hemispheric tropics, vertical profiles of these species show some inversions, that is, increase in concentration with altitude at about 5–15 km altitude that we attribute to the interhemispheric transport mechanism in the model. The extent and frequency of occurrence of these inversions were found to be completely independent of upper boundary conditions. Computed vertical profiles of C_2H_6, C_2H_2, and C_3H_8 compare quite closely to those measured by *Goldman et al.* [1981], *Rudolph et al.* [1981], *Rinsland et al.* [1987], and *Singh et al.* [1988] (not shown here). Figure 11 shows the distribution of percent change in mixing ratios of C_2H_6, C_3H_8, and C_2H_2 for the month of January due to the inclusion of convective transport which is intense in the NH summer. For all three species a small decrease (more than 2%) was calculated in the lowest 2 km in the southern hemispheric tropics due to upward movement of air with high mixing ratios of these compounds and downward movement of air from the free troposphere, which is less concentrated in these species. Because of convective transport, throughout most of the free troposphere, C_2H_6 mixing ratios increased by 5–40%, whereas for C_3H_8 and C_2H_2 the calculated increase ranges between 25–125% and 25–75%, respectively. The difference in the extent of change in mixing ratio distributions of C_2H_6, C_3H_8, and

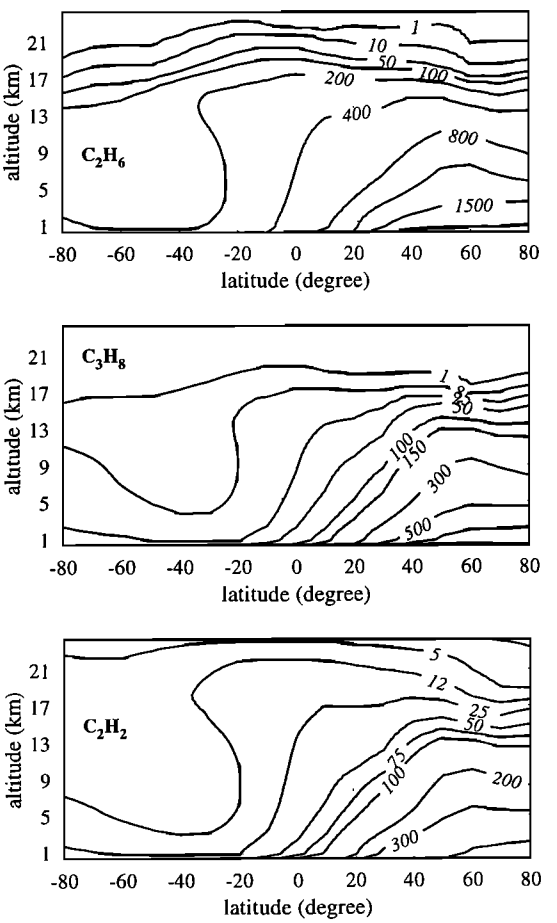

Figure 10. Monthly averaged distributions of C_2H_6, C_3H_8, and C_2H_2 mixing ratios (pptv) in steady state for the month of January calculated using photochemical scheme PC3 and their surface observations shown in Figure 1.

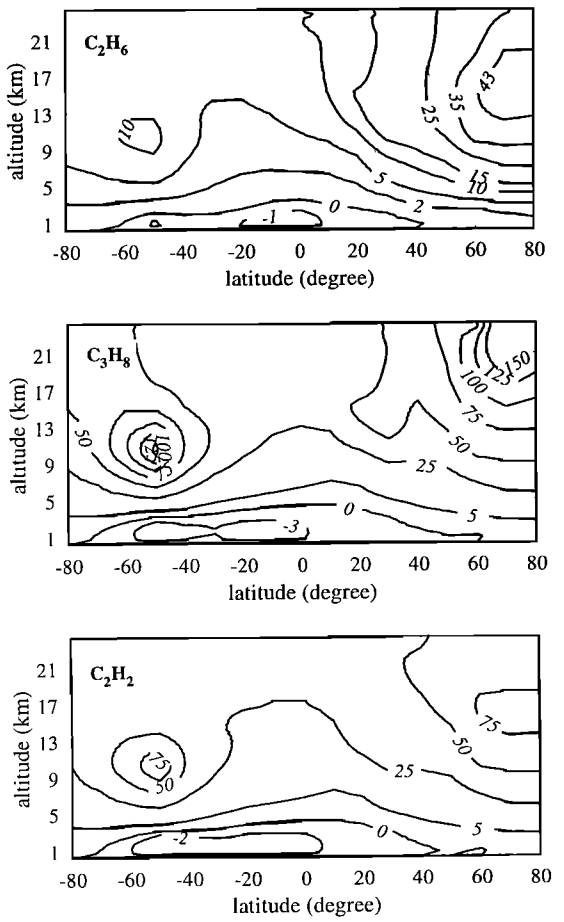

Figure 11. Calculated percent change in monthly averaged mixing ratios of C_2H_6, C_3H_8, and C_2H_2 (shown in Figure 10) for the month of January due to inclusion of convective transport to the photochemical scheme PC3.

C_2H_2 due to convection is entirely governed by the differences in their lifetimes and their concentrations in the PBL. For C_2H_6, because of its longer chemical lifetime, diffusion tends to smooth out the excessive gradient distribution caused by convection. Because our convective transport scheme employs seasonally averaged mass fluxes to be drawn out of the PBL and detrainment profiles, the model does not predict the increase in the mixing ratio of these species with altitude in the NH observed by *N. J. Blake et al.* [1996] which was likely due to episodic convective phenomena.

We have also calculated the steady state global source strength of CH_4 using its surface measurements. For OH fields derived from scheme PC1, the computed emission is 498 Tg/yr with steady state global lifetime of 9.74 years. The ratio of northern hemispheric to southern hemispheric surface emissions for CH_4 is 2.1. Addition of C_2 and C_3 hydrocarbon photochemistry decreased the total surface emission to 490 Tg/yr. Inclusion of convection to scheme PC3 increased this source strength to 500 Tg/yr. Inclusion of soil sinks of CH_4 and CO to scheme PC1 increased the globally averaged OH concentration and resulted in total CH_4 surface emission of 538 Tg/yr, of which 10 Tg/yr is due to chemical feedback between OH and CH_4. These estimates of CH_4 emission are within the range reported by *Cicerone and Oremland* [1988], *Crutzen* [1991], *WMO* [1994], and *IPCC* [1994]. Because of its long lifetime and well-mixed distribution, only a very small increase (<1.0%) in the CH_4 mixing ratio was calculated in the free troposphere due to convection.

6.2. Tetrachloroethene

Tetrachloroethene, C_2Cl_4, is a gas whose only known sources are anthropogenic, although it was suggested that it may have some natural sources from seawater algae [*Abrahamsson et al.*, 1995]. Commercially, C_2Cl_4 is mainly used as a solvent and as a degreasing and dry cleaning agent. In the atmosphere it mainly reacts with OH radicals [*DeMore et al.*, 1997]. Photodissociation in the stratosphere, chlorine-initiated oxidation [*DeMore et al.*, 1997], and oceans [*Pearson and McConnell*, 1975] are other minor sinks of C_2Cl_4. Its global lifetime from reaction with OH radicals is about 4 to 5 months [*Koppmann et al.*, 1993; *Wang et al.*, 1995]. Because of its anthropogenic sources (spatially distributed similar to CFCs and MCF), and its relatively short lifetime, C_2Cl_4 has been suggested as a very useful chemical tracer for the identification of origin of sources and sinks of other trace species [*Rudolph et al.*, 1996; *Singh et al.*, 1996a, b] and for transport mechanisms. Because of its higher sensitivity toward OH radicals, relative to MCF, C_2Cl_4 can be a better indicator of seasonal changes in OH concentration, as suggested by *Wang et al.* [1995]. Using C_2Cl_4, *Rudolph et al.* [1996] and *Singh et al.* [1996c] estimated an upper limit for average tropospheric chlorine radical concentration of the order of (10^2–10^3) molecules cm^{-3}. Oxidation of C_2Cl_4 contributes about 12% to the total production of atmospheric phosgene [*Kindler et al.*, 1995] and 0.5% to the total tropospheric organochlorine [*Wang et al.*, 1995]. Several groups have reported remote surface concentrations of C_2Cl_4 [*Pearson and McConnell*, 1975; *Class and Ballschmitter*, 1986; *Koppmann et al.*, 1993; *Wiedmann et al.*, 1994; *Wang et al.*, 1995].

Here we used the seasonally varying surface mixing ratios of C_2Cl_4 for 1989–1990 of *Wang et al.* [1995]. Using the monthly varying OH radical distribution derived from scheme PC3 and the surface observations, latitudinally varying monthly surface removal rates of C_2Cl_4 are calculated as shown in Figure 12. For this simulation the only sinks of C_2Cl_4 considered are OH radicals for the entire model domain and Cl radicals for the model region between 16.5 and 24.5 km. The calculated annual steady state source strength of C_2Cl_4 is 432 kT with a north to south ratio of 7.5. Of this total chemical loss, about 5% occurs between 16.5 and 24.5 km from chlorine radicals. The steady state corresponding global lifetime of C_2Cl_4 is 3.9 months. This calculated annual source strength differs significantly from 580 kT/yr estimated by *Class and Ballschmitter* [1986] and *Koppmann et al.* [1993] (see Table 4) and 480 kT/yr estimated by *Rudolph et al.* [1996]. For 1990, *Fisher et al.* [1994] estimated 358 kT for global emissions of C_2Cl_4 and speculated that an additional 100 kT/yr of C_2Cl_4 emissions could come from residue processes in developing nations. For the present calculations, latitudinal belts of (30°–60°)N and (20°N–20°S) account for 62 and 24% of its global annual source strength. About 73 kT of the total annual NH source of 381 kT is transported to the SH where it is chemically destroyed, with a maximum amount (11 kT) during January. In steady state the annual SH C_2Cl_4 sink strength is 124 kT.

The calculated annual source strength of C_2Cl_4 is very close to the estimated anthropogenic emission strength averaged for 1989 and 1990. According to *McCulloch and Midgley* [1996], for 1989 and 1990, the global industrial source strengths of C_2Cl_4 are (423 ± 22) kT and (366 ± 19) kT, respectively. Of this total

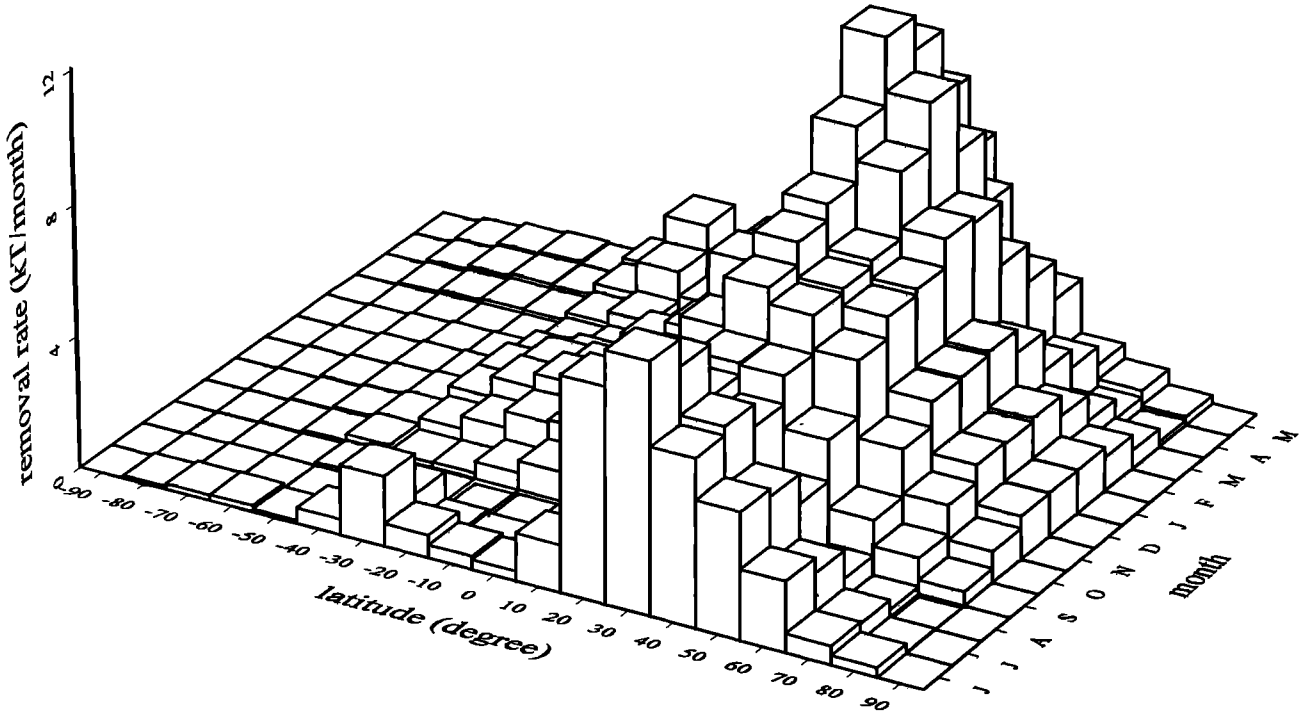

Figure 12. Latitude-time cross section of integrated monthly surface removal rates of C_2Cl_4 per 10° bin in steady state calculated using scheme PC3 and its surface observations.

strength they estimated about 3–4 kT emissions of C_2Cl_4 from the SH. For this estimate to be correct, our model calculation indicates that about 47 kT additional sources of C_2Cl_4 from the SH are needed to satisfy the southern hemispheric mass balance in the steady state. To some extent, this conclusion may depend upon the model structure, chromatographic artifacts, data treatment for the observed surface mixing ratios of C_2Cl_4, and its rate of reaction with OH radicals. There are two possibilities for this required additional source of C_2Cl_4. Either other industrial sources are missing or there are unidentified sources of C_2Cl_4. So far, oceans have been suggested as a natural source [*Abrahamsson et al.*, 1995; *Singh et al.*, 1996c]. *Singh et al.* [1996c] estimated 35 kT/yr, with an upper limit of 70 kT/yr, as the global oceanic source strength of C_2Cl_4. Following the speculation of *Fisher et al.* [1994], some fraction of this missing emission of C_2Cl_4 might come from developing countries.

Inclusion of chlorine oxidation of C_2Cl_4, which at 288 K is 270 times faster than that due to its reaction with OH radicals, in the MBL (assumed to be the lowest model layer) increased the calculated source strength by 17 kT/yr. Adding convective transport to schemes PC1 and PC3 resulted in total calculated annual strengths of 457 and 448 kT, respectively. Owing to its primary emissions in the NH and relatively short lifetime, C_2Cl_4 is most concentrated there, as is evident from its surface measurements (Figure 1) and the simulated distribution using scheme PC3 shown in Figure 13 for the month of July. The calculated mixing ratios of C_2Cl_4 for most of the NH at 13 km range between 3 and 4 ppt, whereas, for the entire SH, C_2Cl_4 mixing ratios are always lower than 3 ppt. Similar to light NMHCs, inclusion of convective transport decreased the C_2Cl_4 mixing ratios by 1% in the lowest 2 km around 20°N and increased its mixing ratios by 10–20% in most of the free northern hemispheric troposphere, as shown in Figure 13.

7. Seasonal Nature of Surface Sources of Light NMHCs

Wang et al. [1995] suggested that C_2Cl_4 could be a sensitive chemical tracer to examine the seasonal amplitude in the hemi-

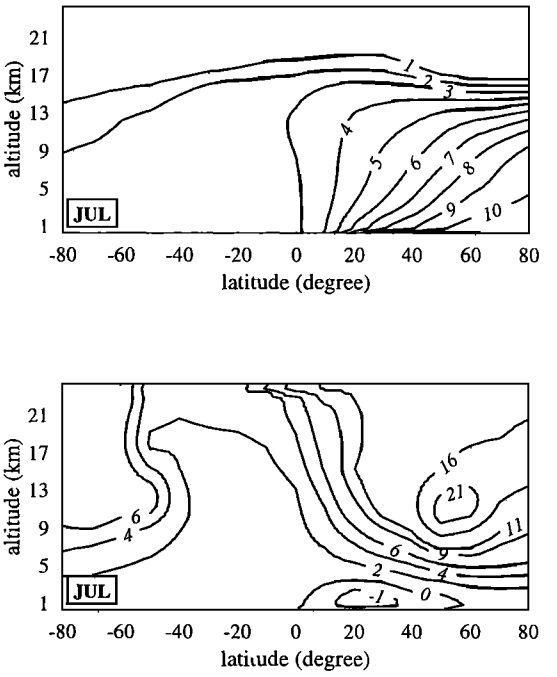

Figure 13. (top) Monthly average distribution of C_2Cl_4 mixing ratios (pptv) in steady state for the month of July calculated using photochemical scheme PC3 and its surface observations shown in Figure 1. (bottom) Also shown is the percent change in this distribution due to the inclusion of convective transport.

spherically averaged OH concentration because major sources of C_2Cl_4 are industrial, while it is primarily destroyed by OH radicals. Moreover, OH radicals are the main sink of surface-emitted light NMHCs which, as shown in section 6, are mostly (>80%) emitted in the NH. Using this information and the conclusion of *McCulloch and Midgley* [1996] that industrial sources of C_2Cl_4 are seasonally independent (and assuming that the calculated minor oceanic source of C_2Cl_4 is also seasonally independent), we have attempted to estimate seasonality in the source strengths of relatively short-lived species C_2H_6, C_3H_8, and C_2H_2. Of these species, C_2H_6 is the longest-lived, and its steady state global lifetime is about one fourth of the model interhemispheric exchange time.

To achieve this objective, we simulated the steady state atmospheric distributions of light NMHCs and C_2Cl_4 using photochemical scheme PC3 (without convection) and their deduced annual source strengths (applied equally per time step) and latitudinal distributions, as described in previous sections, as their lower boundary conditions. For all 12 months the observed and simulated surface mixing ratios of C_2H_6, C_3H_8, C_2H_2, and C_2Cl_4 were hemispherically averaged. For each species the ratios of hemispherically averaged simulated and observed mixing ratios, denoted as S/O, were calculated. For all four species this ratio was found to be different from 1.0, as shown in Table 5. For C_2Cl_4, for the NH during the months of June–October and for the SH during July–October, the ratio S/O exceeded 1.0. Over 1 year, for the northern and southern hemispheres, this ratio varied between 0.79–1.40 and 0.82–1.22, respectively.

In addition to variations in emissions, the observations reflect all dynamical and chemical factors which determine the concentration of a species. Our simulations considered only constant emissions throughout the year in addition to the monthly changes in the interhemispheric exchange rate and OH concentration. Therefore the calculated deviation in values of S/O for C_2Cl_4 from 1.0 should arise from the model's inability to accurately generate the seasonal variations in OH concentration in both hemispheres and interhemispheric exchange. In general, the model has reproduced the general features of OH distributions which, in addition to transport features, have been shown to simulate the observed distributions, north-south gradients, and trends of CFC-11, CFC-12,

Table 5. Ratio (S/O) of Hemispherically Averaged Simulated Steady State Surface Concentrations of Light NMHCs and C_2Cl_4 Using Equal Surface Sources Throughout the Year to Their Corresponding Observed Concentrations

	C_2Cl_4		C_2H_6		C_3H_8		C_2H_2	
Month	NH	SH	NH	SH	NH	SH	NH	SH
Jan.	0.82	0.91	0.81	0.94	0.71	0.79	0.74	0.76
Feb	0.79	0.97	0.82	1.02	0.77	0.97	0.81	0.90
March	0.82	0.95	0.90	1.04	0.88	1.14	0.92	1.01
April	0.92	0.87	1.03	1.04	1.06	1.25	1.11	1.10
May	1.00	0.82	1.16	1.07	1.31	1.42	1.34	1.23
June	1.07	0.88	1.19	1.07	1.52	1.40	1.46	1.31
July	1.17	1.04	1.16	1.03	1.44	1.20	1.34	1.27
Aug.	1.40	1.22	1.22	0.95	1.56	1.00	1.39	1.17
Sept.	1 37	1.22	1.10	0.90	1.09	0.84	1.05	1.01
Oct.	1.07	1.03	0.89	0.89	0.71	0.77	0.72	0.85
Nov.	0.92	0.89	0.78	0.88	0.59	0.69	0.61	0.72
Dec.	0.86	0.84	0.78	0.88	0.62	0.67	0.65	0.67

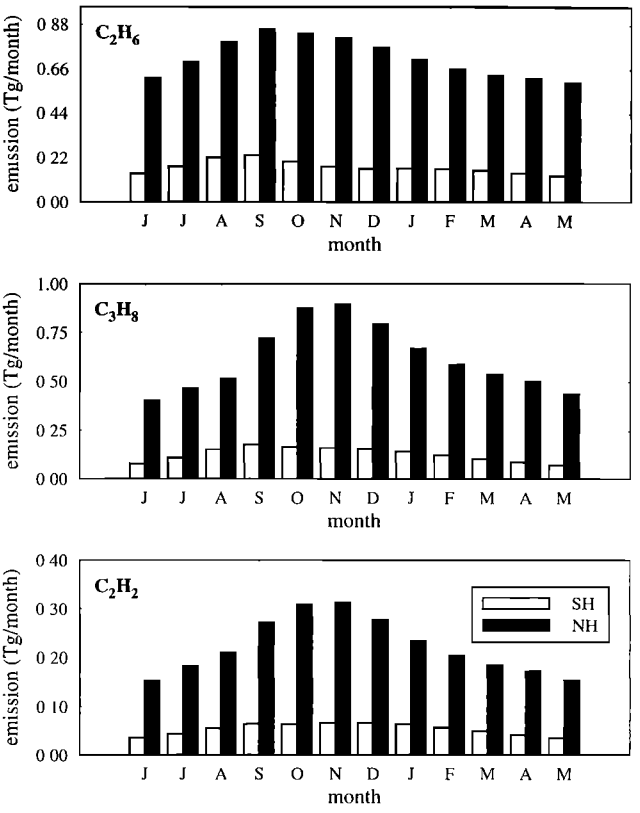

Figure 14. Calculated monthly variations in the hemispheric emissions of C_2H_6, C_3H_8, and C_2H_2 for case PC3A shown in Table 4.

and MCF. Because both of these factors, that is, seasonal variations in OH concentration in both hemispheres and interhemispheric exchange, are equally applicable to C_2Cl_4 and light NMHCs, the calculated deviation in S/O for C_2Cl_4 from 1.0, which will have most contribution due to seasonal variations in OH because of its short lifetime (more than 3 times smaller) as compared to the model interhemispheric exchange time, can be used for each month to normalize the S/O ratios for light NMHCs. This normalization of S/O for light NMHCs with respect to S/O of C_2Cl_4 will cancel the effects of both the factors mentioned before. Therefore any deviation in these normalized ratios for light NMHCs from 1.0 will reflect the seasonality in their sources. This approach should be most accurate for the NMHCs whose atmospheric lifetime is closest to that of C_2Cl_4, that is, C_2H_6, and semiquantitative for other NMHC species. Figure 14 shows the monthly variations in surface source strengths of light NMHCs obtained after multiplying their monthly source strengths with their respective normalized S/O ratios. The calculation shows that emissions of C_2H_6 should be higher than average for the months of August–January in the NH and for July–November in the SH, with maximum amounts during September (0.9 Tg for NH and 0.2 Tg for SH). Emissions of C_3H_8 should be higher than average for the months of September–March in the NH and for August–January in the SH, with maximum amounts during November (0.9 Tg) for the NH and during September (0.2 Tg) for the SH. Similarly, C_2H_2 emissions should be higher than average for the months of September–January in the NH and for August–February in the SH, with maximum amounts during November (0.3 Tg) for the NH and during December (0.1 Tg)

for the SH. These conclusions were unaffected by uniformly changing the surface mixing ratio of C_2Cl_4 by ±25% and introducing the convective transport and repeating the same exercise. To some extent, these conclusions may be affected by the problems associated with background air sampling, the ways that the raw observed data were treated and the hemispheric averaging was performed, and by chromatographic artifacts.

8. Summary

In the present study, we have calculated the global surface removal rates and corresponding latitudinal distributions for CH_4, C_2H_6, C_3H_8, C_2H_2, and C_2Cl_4 using surface measurements from all seasons. The distribution of OH radicals, the primary sink of these hydrocarbons, is photochemically computed using detailed photochemical schemes. For the methane-only model (PC1) the global and annual average OH concentration is 1.0×10^6 molecules cm^{-3}. Annually averaged OH concentrations are found to be higher in the SH which is consistent with some previous studies. Addition of soil sinks for CO and CH_4 and inclusion of NMHC chemistry to photochemical scheme PC1 have significant effects on the global and regional distributions of OH radical and its interhemispheric concentration ratios. Nighttime OH radical concentrations in the lower troposphere were found to be only 40–80 times lower than the daytime maximum value. In the upper troposphere, nighttime OH concentrations drop to almost zero. This difference in diurnal variations in the OH concentration at different altitudes is due to the concentration of HO_2 radicals and their rapid recycling with O_3 and HO_2NO_2.

The annual surface emissions of CH_4, C_2H_6, C_3H_8, C_2H_2, and C_2Cl_4 calculated using the nonconvective scheme PC3 are 490 Tg, 10.4 Tg, 8.4 Tg, 3.1 Tg, and 432 kT, respectively. Inclusion of the convective scheme increased these emission estimates by 2.0, 4.0, 3.9, 4.1, and 3.7%, respectively. For NMHCs and C_2Cl_4 these emissions show distinct latitudinal variations. Because of their relatively short lifetimes compared to the 1 year interhemispheric exchange time, the calculated higher north to south ratios of total emissions of all three NMHCs (which range between 4.0 and 4.7) and C_2Cl_4 (7.5) clearly indicate that more than 80% of their global annual sources originated from the NH. Given the industrial emissions of C_2Cl_4 for the southern hemisphere, estimated by *McCulloch and Midgley* [1996], our calculations indicate that as much as 47 kT of additional southern hemispheric source of C_2Cl_4 is needed for 1989–1990 to attain its steady state mass balance in this region. Because of relatively long lifetimes, these NMHCs and C_2Cl_4 show significant presence in the upper troposphere and lower stratosphere. Modeled increases in southern tropical mixing ratios of these species with altitude in the upper troposphere are explicitly due to the interhemispheric transport feature and not from effects of the upper boundary condition. The calculated atmospheric distributions of NMHCs and C_2Cl_4 are shown to be strongly affected by convective transport.

With the use of C_2Cl_4, which has sources independent of season and also has similar atmospheric chemical sinks as those for NMHCs, the comparison of observed surface mixing ratios of NMHCs with the corresponding modeled surface mixing ratios (calculated using uniform surface emissions throughout the year as the lower boundary condition) indicates that the sources of these species may be seasonal in nature. Over a year, northern hemispheric emissions for C_2H_6, C_3H_8, and C_2H_2 for the months of August–January, September–March, and September–January, respectively, are more than the monthly average emissions.

In future studies we will use these calculated emissions of hydrocarbons to examine the effects of perturbations due to anthropogenic and natural sources of various gases on tropospheric chemical nonlinearity and on the distribution and budgets of key chemical species such as O_3, CO, NO_x, HO_x, and CH_4.

Acknowledgments. Two of us (M.L.G. and R.J.C.) acknowledge support from NASA through award NAGW-4867 and from the INCOR program of the University of California and the Los Alamos National Laboratory. D.R.B. and F.S.R. thank their research group members who collected or assayed samples, modified chromatograms, and compiled the measurement data.

References

Abrahamsson, K., A. Ekdahl, J. Collen, and M. Pedersen, Marine algae—A source of trichloroethylene and perchloroethylene, *Limnol. Oceanogr.*, *40*, 1321–1326, 1995.

Apel, E. C., J. G. Calvert, and F. C. Fehsenfeld, The nonmethane hydrocarbon intercomparison experiment (NOMHICE): Tasks 1 and 2, *J. Geophys. Res.*, *99*, 16,651–16,664, 1994.

Atkinson, R., Gas-phase tropospheric chemistry of organic compounds, *J. Phys. Chem. Ref. Data Monogr.*, *2*, 13–75, 1994.

Atkinson, R., D. L. Baulch, R. A. Cox, R. F. Hampson, J. A. Kerr, and J. Troe, Evaluated kinetic and photochemical data for atmospheric chemistry: Supplement IV, *Atmos. Environ.*, *Part A*, *26*, 1187–1230, 1992.

Barnett, J. J., and M. Corney, A middle atmosphere temperature reference model derived from satellite observations, *Adv. Space Res.*, *5*(7), 125–134, 1985.

Berntsen, T., and I. S. A. Isaksen, A 3-D photochemistry/transport model of the global troposphere, *Rep. 89*, Inst. of Geophys., Univ. of Oslo, Oslo, 1994.

Bey, I., B. Aumont, and G. Toupance, The nighttime production of OH radicals in the continental troposphere, *Geophys. Res. Lett.*, *24*, 1067–1070, 1997.

Blake, D. R., and F. S. Rowland, Global atmospheric concentrations and source strengths of ethane, *Nature*, *321*, 231–233, 1986.

Blake, D. R., and F. S. Rowland, Urban leakage of liquefied petroleum gas and its impact on Mexico City air quality, *Science*, *269*, 953–956, 1995.

Blake, D. R., T. Y. Chen, T. W. Smith Jr., C. J.-L. Wang, O. W. Wingenter, N. J. Blake, F. S. Rowland, and E. W. Mayer, Three-dimensional distribution of nonmethane hydrocarbons and halocarbons over the northwestern Pacific during 1991 Pacific Exploratory Mission (PEM-West A), *J. Geophys. Res.*, *101*, 1763–1778, 1996.

Blake, N. J., D. R. Blake, B. C. Sive, T. Y. Chen, F. S. Rowland, J. E. Collins Jr., G. W. Sachse, and B. E. Anderson, Biomass burning emissions and vertical distribution of atmospheric methyl halides and other reduced carbon gases in the South Atlantic region, *J. Geophys. Res.*, *101*, 24,151–24,164, 1996.

Brenninkmeijer, C. A. M., M. R. Manning, D. C. Lowe, G. Wallace, R. J. Sparks, and A. Volz-Thomas, Interhemispheric asymmetry in OH abundance inferred from measurements of atmospheric ^{14}CO, *Nature*, *356*, 50–52, 1992.

Brice, K. A., and R. G. Derwent, Emissions inventory for hydrocarbons in the United Kingdom, *Atmos. Environ.*, *12*, 2045–2054, 1978.

Chameides, W. L., and R. J. Cicerone, Effects of nonmethane hydrocarbons in the atmosphere, *J. Geophys. Res.*, *83*, 947–952, 1978.

Chameides, W. L., and A. Tan, The two-dimensional diagnostic model for tropospheric OH: An uncertainty analysis, *J. Geophys. Res.*, *86*, 5209–5223, 1981.

Chatfield, R. B., and P. J. Crutzen, Sulfur dioxide in remote oceanic air: Cloud transport of reactive precursors, *J. Geophys. Res.*, *89*, 7111–7132, 1984.

Cicerone, R. J., and R. S. Oremland, Biogeochemical aspects of atmospheric methane, *Global Biogeochem. Cycles*, *2*, 299–327, 1988.

Class, T., and K. Ballschmitter, Chemistry of organic traces in air VI: Distributions of chlorinated C_1-C_4 hydrocarbons in air over the

northern and southern Atlantic Ocean, *Chemosphere*, *15*, 413–427, 1986.

Crutzen, P. J., Role of the tropics in atmospheric chemistry, in *The Geophysiology of Amazonia*, edited by R. E. Dickinson, pp. 107–132, John Wiley, New York, 1987.

Crutzen, P. J., Methane's sinks and sources, *Nature*, *350*, 380–381, 1991.

Crutzen, P. J., and L. T. Gidel, A two-dimensional photochemical model of the atmosphere, 2, The tropospheric budget of the anthropogenic chlorocarbons, CO, CH_4, CH_3Cl, and the effects of various NO_x sources on tropospheric ozone, *J. Geophys. Res.*, *88*, 6641–6661, 1983.

Crutzen, P. J., and P. H. Zimmermann, The changing photochemistry of the troposphere, *Tellus, Ser. AB*, *43*, 136–151, 1991.

Cunnold, D. M., P. J. Fraser, R. F. Weiss, R. G. Prinn, P. G. Simmonds, B. R. Miller, F. N. Alyea, and A. J. Crawford, Global trends and annual releases of CCl_3F and CCl_2F_2 estimated from ALE/GAGE and other measurements from July 1978 to June 1991, *J. Geophys Res.*, *99*, 1107–1126, 1994.

DeMore, W. B., J. J. Margitan, M. J. Molina, R. T. Watson, D. M. Golden, R. F. Hampson, M. J. Kurylo, C. J. Howard, and A. R. Ravishankara, Chemical kinetics and photochemical data for use in stratospheric modeling, *JPL Publ.*, *85-37*, 1985.

DeMore, W. B., S. P. Sander, D. M. Golden, R. F. Hampson, M. J. Kurylo, C. J. Howard, A. R. Ravishankara, C. E. Kolb, and M. J. Molina, Chemical kinetics and photochemical data for use in stratospheric modeling, *JPL Publ.*, *92-20*, 1992.

DeMore, W. B., S. P. Sander, D. M. Golden, R. F. Hampson, M. J. Kurylo, C. J. Howard, A. R. Ravishankara, C. E. Kolb, and M. J. Molina, Chemical kinetics and photochemical data for use in stratospheric modeling, *JPL Publ.*, *97-4*, 1997.

Dickinson, R. E., and R. J. Cicerone, Future global warming from atmospheric trace gases, *Nature*, *319*, 109–115, 1986.

Donahue, N. M., M. K. Dubey, R. Mohrschladt, K. L. Demerjian, and J. G. Anderson, High-pressure flow study of the reactions OH + $NO_x \rightarrow HONO_x$. Errors in the falloff region, *J. Geophys. Res.*, *102*, 6159–6168, 1997.

Duce, R. A., V. A. Mohnen, P. R. Zimmerman, D. Grosjean, W. Cautreels, R. Chatfield, R. Jaenicke, J. A. Ogren, E. D. Pellizzari, and G. T. Wallace, Organic material in the global troposphere, *Rev Geophys.*, *21*, 921–952, 1983

Ehhalt, D H., J. Rudolph, F. Meixner, and U. Schmidt, Measurements of selected C_2-C_5 hydrocarbons in the background troposphere: Vertical and latitudinal variations, *J. Atmos Chem.*, *3*, 29–52, 1985.

Ehhalt, D. H., J. Rudolph, and U. Schimdt, On the importance of light hydrocarbons in multiphase atmospheric systems, in *Chemistry of Multiphase Atmospheric Systems, NATO ASI Ser., Ser. G*, vol. 6, edited by W. Jaeschke, pp. 321–350, Springer-Verlag, New York, 1986.

Ehhalt, D. H., U. Schmidt, R. Zander, P. H. Demoulin, and C. P. Rinsland, Seasonal cycle and secular trend of the total and tropospheric column abundance of ethane above the Jungfraujoch, *J. Geophys. Res.*, *96*, 4985–4994, 1991.

Fehsenfeld, F. C., et al., Emissions of volatile organic compounds from vegetation and the implications for atmospheric chemistry, *Global Biogeochem. Cycles*, *6*, 389–430, 1992.

Field, R. A., M. E. Golstone, J. N. Lester, and R. Perry, The sources and behavior of tropospheric anthropogenic volatile hydrocarbons, *Atmos Environ , Part A*, *26*, 2983–2996, 1992.

Finlayson-Pitts, B. J., Chlorine atoms as a potential tropospheric oxidant in the marine boundary layer, *Res. Chem. Intermed.*, *19*, 235–249, 1993.

Fisher, D. A., T. Duafala, P. M. Midgley, and C. Niemi, Production and emission of CFCs, halons and related molecules, *NASA Ref. Publ.*, *1339*, 1994.

Fuglestvedt, J. S., T. K. Berntsen, and I. S. A. Isaksen, Responses in tropospheric O_3, OH and CH_4 to changed emissions of important trace gases, *Report 1993:4*, CICERO, Univ. of Oslo, Oslo, Norway, 1993.

Goldman, A., F. J. Murcray, R. D. Blatherwick, J. R. Gillis, F. S. Bonomo, F. H. Murcray, D. G. Murcray, and R. J. Cicerone, Identification of acetylene (C_2H_2) in infrared atmospheric absorption spectra, *J. Geophys. Res.*, *86*, 12,143–12,146, 1981.

Guenther, A., et al., A global model of natural volatile organic compound emissions, *J. Geophys. Res.*, *100*, 8873–8892, 1995.

Gupta, M. L., Modeling the role of selected light nonmethane hydrocarbons on the chemical composition of natural and perturbed troposphere, Ph.D. dissertation, Univ. of Calif., Irvine, 1996.

Gupta, M. L., S. Tyler, and R. Cicerone, Modeling atmospheric $\delta^{13}CH_4$ and the causes of recent changes in atmospheric CH_4 amounts, *J. Geophys. Res.*, *101*, 22,923–22,932, 1996.

Gupta, M. L., M. P. McGrath, R. J. Cicerone, F. S. Rowland, and M. Wolfsberg, $^{12}C/^{13}C$ kinetic isotope effects in the reactions of CH_4 with OH and Cl, *Geophys. Res. Lett.*, *24*, 2761–2764, 1997.

Hegg, D. A., L. F. Radke, P. V. Hobbs, and R. A. Rasmussen, Emissions of some trace gases from biomass fires, *J. Geophys. Res.*, *95*, 5669–5675, 1990.

Hesstvedt, E., Ø. Hov, and I. S. A. Isaksen, Quasi-steady-state approximations in air pollution modeling: Comparison of two numerical schemes for oxidant prediction, *Int. J. Chem. Kinet.*, *5*, 971–994, 1978.

Hough, A. M., Development of a two-dimensional global tropospheric model: Model chemistry, *J. Geophys. Res.*, *96*, 7325–7362, 1991.

Intergovernmental Panel on Climate Change (IPCC), *Climate Change*, Cambridge Univ. Press, New York, 1994.

IPCC, *Climate Change*, Cambridge Univ. Press, New York, 1995.

Isaksen, I. S. A., Is the oxidizing capacity of the atmosphere changing? in *The Changing Atmosphere*, edited by F. S. Rowland and I. S. A. Isaksen, pp. 141–170, Wiley-Interscience, New York, 1988.

Isaksen, I. S. A., and Ø. Hov, Calculations of trends in the tropospheric concentrations of O_3, OH, CO, CH_4, and NO_x, *Tellus, Ser B*, *39*, 271–285, 1987.

Isaksen, I. S. A., and H. Rhode, A two-dimensional model for the global distribution of gases and aerosol particles in the troposphere, *Rep. AC-47*, Dep. Meteorol., Univ. Stockholm, Stockholm, 1978.

Isaksen, I. S. A., and F. Stordal, Ozone perturbations by enhanced levels of CFCs, N_2O, and CH_4: A two-dimensional diabatic circulation study including uncertainty estimates, *J. Geophys Res.*, *91*, 5249–5263, 1986.

Isaksen, I. S. A., K. H. Midtbø, J. Sunde, and P. J. Crutzen, A simplified method to include molecular scattering and reflection in calculations of photon fluxes and photodissociation rates, *Geophys. Norv.*, *31*, 11, 1977.

Isaksen, I. S A., Ø. Hov, S. A. Penkett, and A. Semb, Model analysis of the measured concentration of organic gases in the Norwegian Arctic, *J. Atmos. Chem.*, *3*, 3–27, 1985.

Jonson, J. E., and I. S. A. Isaksen, The impact of solar flux variations on the tropospheric ozone chemistry, *Rep 81*, Inst. of Geophys., Univ. of Oslo, Oslo, 1991.

Kaiser, E. W., and T. J. Wellington, Pressure dependence of the reaction Cl + C_3H_6, *J. Phys. Chem.*, *100*, 9788–9793, 1996.

Kanakidou, M., B. Bonsang, J. C. Le Roulley, D. Martin, and G. Sennequier, Marine source of atmospheric acetylene, *Nature*, *333*, 51–52, 1988.

Kanakidou, M., B. Bonsang, and G. Lambert, Light hydrocarbons vertical profiles and fluxes in a French rural area, *Atmos. Environ.*, *23*, 921–927, 1989.

Kanakidou, M., H. B. Singh, K. M. Valentin, and P. J. Crutzen, A two-dimensional study of ethane and propane oxidation, *J. Geophys. Res.*, *96*, 15,395–15,413, 1991a.

Kanakidou, M., P. J. Crutzen, P. H. Zimmermann, and B. Bonsang, A 3 dimensional global study of the photochemistry of ethane and propane in the troposphere: Production and transport of organic nitrogen compounds, paper presented at the NATO/CCMS 19th ITM on Air Pollution Modeling and its Applications, Ierapetra, Greece, Sept. 29 to Oct. 4, 1991b.

Keene, W. C., D. J. Jacob, and S.-M. Fan, Reactive chlorine: A potential sink for dimethylsulfide and hydrocarbons in the marine boundary layer, *Atmos. Environ.*, *30*, 1–3, 1996.

Kindler, T. P., W. L. Chameides, P. H. Wine, D. M. Cunnold, F. N. Alyea, and J. A. Franklin, The fate of atmospheric phosgene and stratospheric chlorine loadings of its parent compounds: CCl_4, C_2Cl_4, C_2HCl_3, CH_3CCl_3, and $CHCl_3$, *J. Geophys. Res.*, *100*, 1235–1251, 1995.

Koppmann, R., F. J. Johnen, C. Plass-Dulmer, and J. Rudolph, Distribution of methylchloride, dichloromethane, trichloroethane, and tetrachloroethene over the North and South Atlantic, *J. Geophys. Res.*, *98*, 20,517–20,526, 1993.

Lacis, A. A., D. J. Wuebbles, and J. A. Logan, Radiative forcing of climate by changes in the vertical distribution of ozone, *J. Geophys Res.*, *95*, 9971–9981, 1990.

Lamb, B., A. Guenther, D. Gay, and H. Westberg, A national inven-

tory of biogenic hydrocarbon emissions, *Atmos. Environ.*, *21*, 1695–1705, 1987.

Langner, J., H. Rodhe, and M. Olofsson, Parametrization of subgrid scale vertical tracer transport in a global two-dimensional model of the troposphere, *J. Geophys. Res.*, *95*, 13,691–13,706, 1990.

Lelieveld, J., and P. J. Crutzen, Role of deep cloud convection in the ozone budget of the troposphere, *Science*, *264*, 1759–1761, 1994.

Lin, X., M. Trainer, and S. C. Liu, On the nonlinearity of ozone production, *J. Geophys. Res.*, *93*, 15,879–15,888, 1988.

Liu, S. C., M. Trainer, F. C. Fehsenfeld, D. D. Parrish, E. J. Williams, D. W. Fahey, G. Hubler, and P. C. Murphy, Ozone production in the rural troposphere and the implications for regional and global ozone distributions, *J. Geophys. Res.*, *92*, 4191–4207, 1987.

Lu, Y., and M. A. K. Khalil, Tropospheric OH: Model calculations of spatial, temporal, and secular variations, *Chemosphere*, *23*, 397–444, 1991.

McCulloch, A., and P. M. Midgley, The production and global distribution of emissions of trichloroethene, tetrachloroethene and dichloromethane over the period 1988–1992, *Atmos. Environ.*, *30*, 601–608, 1996.

Mihelcic, D., D. Klemp, P. Musgen, H. W. Patz, and A. Volz-Thomas, Simultaneous measurements of peroxy and nitrate radicals at Schauinsland, *J. Atmos. Chem.*, *16*, 313–335, 1993.

Muller, J.-F., Geographical distribution and seasonal variation of surface emissions and deposition velocities of atmospheric trace gases, *J. Geophys. Res.*, *97*, 3787–3804, 1992.

Nelson, P. F., S. M. Quigley, and M. Y. Smith, Sources of atmospheric hydrocarbons in Sydney: A quantitative determination using a source reconciliation technique, *Atmos. Environ.*, *17*, 439–449, 1983.

Pearson, C. R., and G. McConnell, Chlorinated C_1 and C_2 hydrocarbons in the marine environment, *Proc. R. Soc. London, Ser. B.*, *189*, 305–322, 1975.

Penkett, S. A., Non-methane organics in the remote troposphere, in *Atmospheric Chemistry*, edited by E. D. Goldberg, pp. 329–355, Springer-Verlag, New York, 1982.

Piccot, S. D., J. J. Watson, and J. W. Jones, A global inventory of volatile organic compound emissions from anthropogenic sources, *J. Geophys. Res.*, *97*, 9897–9912, 1992.

Pinto, J. P., Y. L. Yung, D. Rind, G. L. Russell, J. A. Lerner, J. E. Hansen, and S. Hameed, A general circulation model study of atmospheric carbon monoxide, *J. Geophys. Res.*, *88*, 3691–3702, 1983.

Plass-Dulmer, C., R. Koppmann, M. Ratte, and J. Rudolph, Light nonmethane hydrocarbons in seawater, *Global Biogeochem. Cycles*, *9*, 79–100, 1995.

Platt, U., L. LeBras, G. Poulet, J. P. Burrows, and G. Moortgat, Peroxy radicals from nighttime reaction of NO_3 with organic compounds, *Nature*, *348*, 147–149, 1990.

Plumb, R. A., and J. D. Mahlman, The zonally averaged transport characteristics of the GFDL general circulation/transport model, *J. Atmos. Sci.*, *44*, 298–327, 1987.

Prather, M. J., and C. M. Spivakovsky, Tropospheric OH and the lifetimes of hydrochlorofluorocarbons, *J. Geophys. Res.*, *95*, 18,723–18,729, 1990.

Prinn, R. G., The interactive atmosphere: Global atmospheric-biospheric chemistry, *Ambio*, *23*, 50, 1994.

Prinn, R., D. M. Cunnold, R. A. Rasmussen, P. G. Simmonds, F. N. Alyea, A. J. Crawford, P. J. Fraser, and R. D. Rosen, Atmospheric trends in methylchloroform and the global average for the hydroxyl radical, *Science*, *238*, 945–950, 1987.

Prinn, R. G., R. F. Weiss, B. R. Miller, J. Huang, F. N. Alyea, D. M. Cunnold, P. J. Fraser, D. E. Hartley, and P. G. Simmonds, Atmospheric trends and lifetime of CH_3CCl_3 and global OH concentration, *Science*, *269*, 187–192, 1995.

Ramanathan, V., R. J. Cicerone, H. B. Singh, and J. T. Kiehl, Trace gas trends and their potential role in climate change, *J. Geophys. Res.*, *90*, 5547–5566, 1985.

Rinsland, C. P., R. Zander, C. B. Farmer, R. H. Norton, and J. M. Russell III, Concentrations of ethane (C_2H_6) in the lower stratosphere and upper stratosphere and acetylene (C_2H_2) in the upper stratosphere deduced from atmospheric trace molecule spectroscopy/Spacelab 3 spectra, *J. Geophys. Res.*, *92*, 11,951–11,964, 1987.

Roemer, M. G. M., and K. D. van den Hout, Emission of NMHCs and NO_x and global ozone production, *TNO-Rep. P 91/025*, TNO Inst. of Environ. Sci., Netherlands, 1991.

Rudolph, J., The tropospheric distribution and budget of ethane, *J. Geophys. Res.*, *100*, 11,369–11,381, 1995.

Rudolph, J., D. H. Ehhalt, and A. Tonnissen, Vertical profiles of ethane and propane in the stratosphere, *J. Geophys. Res.*, *86*, 7267–7272, 1981.

Rudolph, J., D. H. Ehhalt, and A. Khedim, Vertical profiles of acetylene in the troposphere and stratosphere, *J. Atmos. Chem.*, *2*, 117–124, 1984.

Rudolph, J., R. Koppmann, and C. Plass-Dulmer, The budgets of ethane and tetrachloroethene: Is there evidence for an impact of reactions with chlorine atoms in the atmosphere? *Atmos. Environ.*, *30*, 1887–1894, 1996.

Seiler, W., and R. Conrad, Contribution of tropical ecosystems to the global budgets of trace gases, especially CH_4, H_2, CO and N_2O, in *The Geophysiology of Amazonia*, edited by R. E. Dickinson, pp. 107–160, John Wiley, New York, 1987.

Sillman, S., J. A. Logan, and S. C. Wofsy, The sensitivity of ozone to nitrogen oxides and hydrocarbons in regional ozone episodes, *J. Geophys. Res.*, *95*, 1837–1851, 1990.

Singh, H. B., and J. F. Kasting, Chlorine-hydrocarbon photochemistry in the marine troposphere and lower stratosphere, *J. Atmos. Chem.*, *7*, 261–285, 1988.

Singh, H. B., and P. B. Zimmerman, Atmospheric distribution and sources of nonmethane hydrocarbons, *Adv. Environ. Sci. Technol.*, *24*, 177–235, 1992.

Singh, H. B., W. Viezee, and L. J. Salas, Measurements of selected C_2-C_5 hydrocarbons in the troposphere: Latitudinal, vertical, and temporal variations, *J. Geophys. Res.*, *93*, 15,861–15,878, 1988.

Singh, H. B., D. O'Hara, D. Herlth, W. Sachse, D. R. Blake, J. D. Bradshaw, M. Kanakidou, and P. J. Crutzen, Acetone in the atmosphere: Distribution, sources, and sinks, *J. Geophys. Res.*, *99*, 1805–1819, 1994.

Singh, H. B., et al., Reactive nitrogen and ozone over the western Pacific: Distribution, partitioning, and sources, *J. Geophys. Res.*, *101*, 1793–1808, 1996a.

Singh, H. B., et al., Low ozone in the marine boundary layer of the tropical Pacific Ocean: Photochemical loss, chlorine atoms, and entrainment, *J. Geophys. Res.*, *101*, 1907–1917, 1996b.

Singh, H. B., A. N. Thakur, Y. E. Chen, and M. Kanakidou, Tetrachloroethylene as an indicator of low Cl atom concentrations in the atmosphere, *Geophys. Res. Lett.*, *23*, 1529–1532, 1996c.

Smith, T. W., Summertime tropospheric nonmethane hydrocarbon and halocarbon concentrations over central and eastern Canada during ABLE-3B, Ph.D. dissertation, Univ. of Calif., Irvine, 1993.

Spivakovsky, C. M., R. Yevich, J. A. Logan, S. C. Wofsy, and M. B. McElroy, Tropospheric OH in a three-dimensional chemical tracer model: An assessment based on observations of CH_3CCl_3, *J. Geophys. Res.*, *95*, 18,441–18,471, 1990.

Stordal, F., I. S. A. Isaksen, and K. Horntveth, A diabatic circulation two-dimensional model with photochemistry: Simulations of ozone and long-lived tracers with surface sources, *J. Geophys. Res.*, *90*, 5757–5776, 1985.

Strand, A., and Ø. Hov, A two-dimensional study of tropospheric ozone production, *J. Geophys. Res.*, *99*, 22,877–22,895, 1994.

Tanner, D. J., and F. L. Eisele, Present OH measurement limits and associated uncertainties, *J. Geophys. Res.*, *100*, 2883–2892, 1995.

Taylor, J. A., G. P. Brasseur, P. R. Zimmerman, and R. J. Cicerone, A study of the sources and sinks of methane and methyl chloroform using a global three-dimensional lagrangian tropospheric tracer transport model, *J. Geophys. Res.*, *96*, 3013–3044, 1991.

Thompson, A. M., The oxidizing capacity of the Earth's atmosphere: Probable past and future changes, *Science*, *256*, 1157–1165, 1992.

Tie, X., C.-Y. Kao, E. J. Mroz, R. J. Cicerone, F. N. Alyea, and D. M. Cunnold, Three-dimensional simulations of atmospheric methyl chloroform: Effect of an ocean sink, *J. Geophys. Res.*, *97*, 20,751–20,769, 1992.

Tille, K. J. W., M. Savelsberg, and K. Bächmann, Airborne measurements of nonmethane hydrocarbons over western Europe: Vertical distributions, seasonal cycles of mixing ratios and source strengths, *Atmos. Environ.*, *19*, 1751–1760, 1985.

Wang, J.-L., D. R. Blake, and F. S. Rowland, Season variation in the atmospheric distribution of a reactive chlorine compound, tetrachloroethene (CCl_2=CCl_2), *Geophys. Res. Lett.*, *22*, 1097–1100, 1995.

Weiss, W., A. Sittkus, H. Stockburger, and H. Sartorius, Large-scale atmospheric mixing derived from meridional profiles of Krypton 85, *J. Geophys. Res.*, *88*, 8574–8578, 1983.

Whitby, R. A., and E. R. Altwicker, Acetylene in the atmosphere:

Sources representative ambient concentrations and ratios to other hydrocarbons, *Atmos. Environ.*, *12*, 1289–1296, 1978.

Wiedmann, T. O., B. Guthner, T. J. Class, and K. Ballschmitter, Global distribution of tetrachloroethene in the troposphere: Measurements and modeling, *Environ. Sci. Technol.*, *28*, 2321–2329, 1994.

Wingenter, O. W., M. K. Kubo, N. J. Nicola, T. W. Smith Jr., D. R. Blake, and F. S. Rowland, Hydrocarbon and halocarbon measurements as photochemical and dynamical indicators of atmospheric hydroxyl, atomic chlorine, and vertical mixing obtained during Lagrangian flights, *J. Geophys. Res.*, *101*, 4331–4340, 1996.

World Meteorological Organization (WMO), Scientific assessment of ozone depletion: 1994, *Rep. 37*, Geneva, 1994.

R. Cicerone, Department of Earth System Science, University of California, Irvine, CA 92697. (e-mail: rjcicero@uci.edu)

D. Blake and F. S. Rowland, Department of Chemistry, University of California, Irvine, CA 92697. (e-mail: drblake@uci.edu; rowland@uci.edu)

M. Gupta, Department of Atmospheric Sciences, University of California, Los Angeles, CA 90095. (e-mail: gupta@atmos.ucla.edu)

I. Isaksen, Institute of Geophysics, University of Oslo, P. O. Box 1022, Blindern, N-0315, Oslo, Norway. (e-mail: ivar.isaksen@geophysikk.uio.no)

(Received January 15, 1998; revised July 31, 1998; accepted August 10, 1998.)